Chapter 5 Application of the Feedforward Filtered-X LMS Algorithm to the Active Control of Sound in a Ford Explorer

In the previous chapter, general results for control in a three dimensional cavity have been presented. It was shown that global control is possible at frequencies where the number of modes that contribute to the response is lower than the number of control sources. In this chapter, the application of active noise control in the cabin of a Ford Explorer donated by Ford Motor Co. is discussed. Issues relative to the experimental implementation of the system will be addressed.

The test vehicle is shown in Figure 5.1. There are three main types of noise disturbance in an automobile cabin. Their importance depends on the use of the automobile. The noise due to the power train, is dominant when the car is driven on a steep road or if the engine speed is increased. The road noise is dominant when the car is driven on a rough road. In certain conditions wind noise may become a problem, however it has never been the case with the test vehicle. The active noise control strategy was applied to two types of noise problems, noise due to the power train and noise due to the interaction of the tires with the road surface. For these two types of noise problems, accelerometers were used as reference sensors, microphones as error sensors, and speakers created the secondary pressure field. Two types of speakers were investigated. The first set of experiments was conducted using commercially-available loudspeakers. However, the standard speakers and amplifiers preinstalled in the automobile were replaced with top end Alpine System. The second set of experiments was conducted using advanced prototype lightweight and compact piezoelectric speakers. These speakers are

discussed in more detail in section 5.2.4. In all the experiments conducted in this chapter the signals from the microphones are presented in dB A. The error sensors used in the controller are directly input in dB A. This weighting function has been chosen because it takes into account the sensitivity of the human ear.

In section 5.1, a method for selecting reference signals is presented. This method predicts the maximum attenuation achievable by the controller at the error sensor, and it is based on the multiple coherence between potential reference signals and the error sensor signal.

In section 5.2 results of active control of power train noise with optimized reference sensor placement are presented. Numerous experiments were performed for different configurations of actuators and sensors. The effects of the control, both at the error sensors and also in terms of spatial distribution in the cabin were investigated.

In section 5.3, attention is drawn towards the problem of active control of cabin noise due to the interaction of the tires with the road surface. Before the location of the reference sensors was optimized, a principal component analysis was performed while the car was driven on a rough road. This analysis determined the number of independent sources that contribute to the response at the error sensor in the cabin. Preliminary results of active noise control involving four reference accelerometers, one actuator, and one error signal are presented.

Figure 5.1 General view of the car

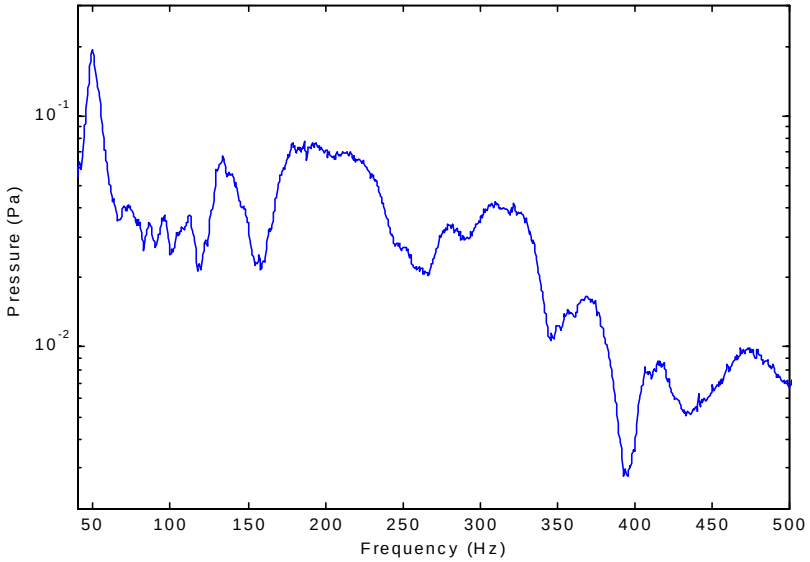

(a) Magnitude of the Frequency Response function

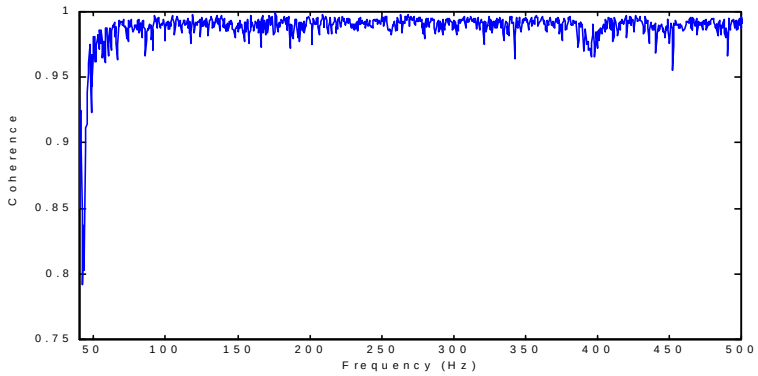

(b) Coherence

Figure 5.2 Transfer function between the input voltage to the speaker and a microphone located at the passenger's head.

Knowledge of the acoustic dynamics of the interior cabin is very important for an accurate determination of the number of sources required to achieve global control of the cabin pressure field. Figure 5.2 shows the transfer function between the input voltage to a speaker located in the trunk of the automobile (random noise band pass filtered between 40 and 500 Hz) and an error microphone sensor located at the head level of the passenger. Obviously, the cabin is acoustically highly damped. Nevertheless, the first resonant frequency (mode 1) distinctly appears at 50 Hz, as seen in Figure 5.2 (a). As it was shown in the test cavity, this mode has a

nodal plane in its center (Figure 3.6 (a)), and the pressure reaches a maximum close to the front panels of the cavity (by analogy, in the automobile the pressure reaches a maximum close to the windshield). This implies that the sound pressure level is high around the heads of the driver and passenger compared, to the rest of the cabin. It is therefore very important to control this mode. This mode is known as the vehicle 'boom' mode. As shown in Figure 5.2 (a). The dynamics of the interior cabin of the car is somewhat different from the dynamics of the test cavity Figure 3.12). The damping associated with each mode is higher in the automobile cabin than in the test cavity. In the test cavity, there are fifteen modes between 150 Hz and 250 Hz. Due to the similarities in shape and dimensions between the test cavity and the automobile, the number of acoustic modes existing in the cabin is also fifteen in the same frequency band. This implies that many modes contribute to the response at frequencies higher than 50 Hz. Considering the conclusions drawn in chapter 4, global control of the pressure field inside the cabin requires a high number of control sources. The present controller available at the Vibration and Acoustics Laboratories in Virginia Tech supports only four control actuators. Because the number of degrees of freedom of the sound pressure field is greater than four in the frequency band considered, a more sensible goal is to create a zone of quiet as large as possible around the error sensors, in the regions where noise reduction is most important e.g., near the passenger's head.

5.1 A Method for Reference Signal Selection

The main difference between the case of the test structure presented in chapter four, and the case of the car, is the exact knowledge of the disturbance signal. As it has been described in the previous chapter, in the case of the test structure, the shaker receives a band pass signal from a white noise generator. This implies two important features for the controller: first, perfect knowledge of the disturbance for the reference signal, and second, the pressure field in the test cavity is limited in frequency. In the automobile the problem is more complicated. When the disturbance is caused by the power train, there are many sources that radiate noise into the cabin. It is difficult to analyze these sources because the acoustic and structural paths are complex. Determination of appropriate reference signals is not straightforward. The method for reference signal selection, based on multiple coherence, is discussed here. Also, it is important to

remember that the control bandwidth of interest presented here is limited in the frequency domain between 40 and 500 Hz, while the frequency content of the disturbance is not limited to this same band. Thus, extensive use of Ithaco filters is required to band pass filter the signals coming from the reference accelerometers, the error sensors, and those going to the control actuators, as illustrated in Figure 5.3. The control was limited to frequencies below 500 Hz for two reasons. Active noise control works best at low frequencies, as discussed in chapter 1; the energy of the disturbances such as power train and road noise are concentrated in frequencies below 500 Hz.

The goal of this section is to show how the performance of the control is related to the coherence between the signal from the error sensors and the signals from the accelerometers located at different positions in the car, and what it implies in terms of noise reduction.

According to [4], the coherence function can be expressed as follows for each frequency:

$$\gamma_{xy}^2 = \frac{S_{xy}^H S_{xx}^{-1} S_{xy}}{S_{yy}}, \qquad (5.1)$$

where S_{xy} is the vector of cross-spectral density between each reference signal and the signal from the error sensor, S_{xx} is the matrix of cross-spectral density between the reference signals, and S_{yy} is the power spectral density of the signal from the error sensor. A total measured output spectrum, S_{yy}, is the result of an ideal linear output, S_{vv} (coherent output), and output noise S_{nn}. The coherent output can be expressed in terms of the coherence as follows:

$$S_{vv} = \gamma_{xy}^2 S_{yy}. \qquad (5.2)$$

The coherence output can be interpreted as the portion of the output, which is linearly due to the input. In the case of a feed-forward control, it represents the fraction of the output, which can be controlled. The incoherent output, S_{nn}, is uncontrollable. It can be expressed in terms of the coherence function and the total output spectrum:

$$S_{nn} = (1 - \gamma_{xy}^2) S_{yy} . \qquad (5.3)$$

S_{nn} represents the minimal remaining noise if active noise control is used with the reference signals that have a coherence γ_{xy} with the total output S_{yy}. Table 5.1 shows the attenuation obtained for some typical coherence values calculated with Equation (5.3). The coherence

function will therefore be used to determine which reference signals are appropriate as well as their number.

Table 5.1 Example attenuation in terms of the coherence

Coherence	Attenuation
0.99	20 dB
0.95	13 dB
0.9	10 dB
0.8	7 dB

The experimental procedure is as follows. The signals of the reference sensors, as well as the signals from the error sensors located in the cabin, are band pass filtered between 40 and 500 Hz, using Ithaco filters. The filtered signal is then recorded for 10 seconds (in order to average the data 10 times and keep one hertz resolution during the post processing) at a sampling frequency of 2048 Hz (four times the upper frequency limit) using an acquisition system linked to a PC. The time history data are post-processed using MATLAB CSD (cross spectral density) and PSD (power spectral density) functions [50]. The coherence and minimized sound were evaluated using equations (5.1) and (5.3) respectively. The set up used to acquire the time domain data is illustrated in Figure 5.3.

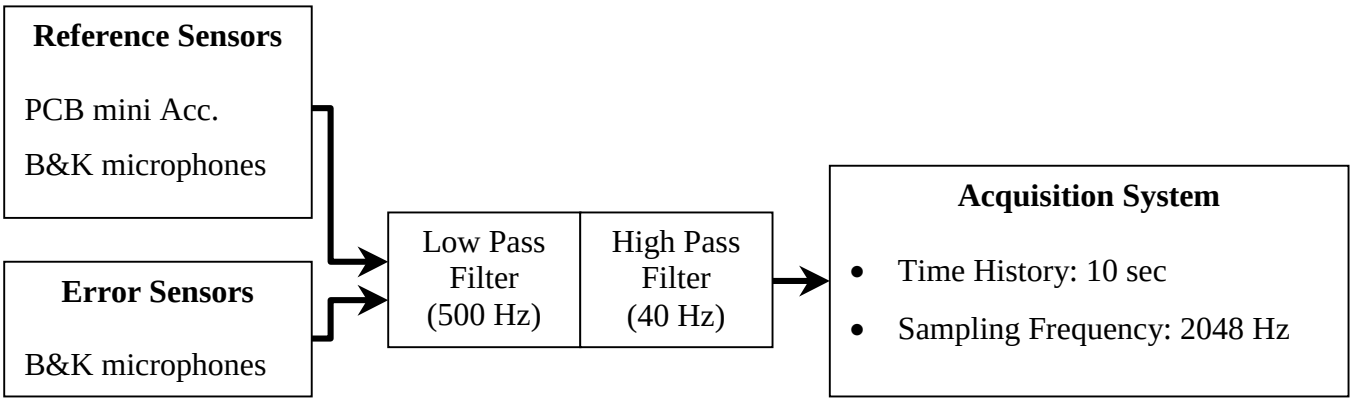

Figure 5.3 Acquisition system set-up.

5.2 Active Noise Control of Power Train Noise

Active noise control of the power train noise was performed for several configurations of actuators and error sensor. The algorithm is a feed-forward filtered-X LMS, used as a broad band controller between 40 and 500 Hz. The frequency band was chosen because the energy of the signals associated with the power train noise decays quickly at higher frequencies.

In section 5.2.1, the method presented in section 5.1 for selection of the reference sensor locations is applied to the case of power train noise.

After a brief description of the test set-up in section 5.2.2, results are presented for cases where the automobile was in the laboratory, with the engine turning at 2900 rpm. This engine speed was chosen in order to obtain a clean frequency response (computed at microphones inside the automobile cabin) with the harmonics of the firing frequency 10 dB above the background noise. The characteristics of the frequency are shown in Figure 5.6 and discussed in the next section. The control was performed for various configurations of commercially available speakers. The control was also performed when the car was driven at constant speed on a steep road. For this particular test, the engine speed was 4300 rpm and the results are presented in section 5.2.4. This engine speed was chosen such that power train noise is dominant relative to the noise of other cars as well as road and aerodynamic noises. Results obtained in the laboratory environment (section 5.2.3) will be compared to the results obtained on the road in order to validate the procedure. After validation of the laboratory tests, results of control using the piezoelectric speakers, performed in the laboratory environment with the engine turning, will be presented (section 5.2.5).

5.2.1 Optimization of the location of the reference sensors

As illustrated in Figure 5.4, different candidate reference signals have been investigated. They can be classified into two distinct categories:

- Those directly connected to the engine (Figure 5.4): accelerometers glued on the engine mount, on the oil fill stem, as well as the signal from the tachometer and a microphone.

- Those glued to the body of the car: the vibration of the engine and power train induces the vibration of other components of the car. Each component connection induces non-linearity. As a result, the vibration of the firewall and body of the car, which radiate sound into the cabin, are not linearly related to the vibration of the engine. Therefore, the reference sensors previously described are not sufficient to characterize the sound pressure measured by a microphone located inside the automobile cabin.

The coherence function (γ^2), together with the estimate of the remaining noise after control (S_{nn}), were computed using equations (5.1) and (5.3) in the frequency range of interest (40-500Hz) for different configurations of reference signals. The most significant results are presented in Table 5.2 and Figures 5.5 to 5.12.

As illustrated in Figure 5.6, the pressure measured at the error sensor is multi-harmonic. The engine rotation speed and particularly the firing frequency of the cylinders determine the fundamental frequency of the signal. When the engine is running at 3300 rpm ($\frac{3300rpm}{60s/\min} = 55rps^{1} = 55Hz$), the firing frequency is 22.5 Hz (one half of engine speed). At the predominant frequency (110 Hz), the amplitude of the response at the harmonic varies from 30 dB above the background noise of the engine down to 5 dB at secondary frequencies (275 Hz).

In the case of six reference signals, good coherence (above 0.99) was obtained at the harmonics of the firing frequencies of the cylinder (Figure 5.5). At other frequencies, where the sound pressure level is low before control, the coherence drops and very little control was achieved. For instance, the coherence was close to 0.3 at 250 Hz, which corresponds to negligible attenuation. Nevertheless, some control was achieved off peak, which decreased the background noise of the engine a couple of decibels on a large frequency band as illustrated in Figure 5.6. The background noise of the engine is defined as the noise off-peak (25 dB A at 250 Hz in Figure 5.6). In fact, the total reduction at the error sensor was 12 dB in the 40-500 Hz band, while the maximum peak reduction at 110 Hz was 31 dB.

The number position and attenuation for each configuration discussed in this section are given in Table 5.2. Note from the table that as the number of reference signals was decreased, the global attenuation decreased also. Reductions of 9.7 (configuration 2), 8.7 (configuration 3)

[1] rps = revolutions per second

down to 4.5 dB (configuration 8) were obtained respectively with four, three and one reference signal. The same trend was also seen for the peak reduction. As illustrated in Figures 5.8 to 5.10, using three reference sensors correctly positioned, good coherence (above 0.9) was obtained for all the harmonics of the firing frequency, and a maximum peak reduction of 25 dB was achieved (table 5.2; **3**). In fact all the peaks were cancelled when this configuration of reference signals was used (less than one decibel above the background noise of the engine) as shown in Figure 5.10. Nevertheless, very little off-peak reduction was obtained. In the case where only one reference sensor was used, a 17 dB peak attenuation was achieved at one harmonic and 13 dB at the others (table 5.2; **8**). Although the tachometer signal was thought to be a good reference signal, as shown in Figure 5.12 good coherence was obtained for only two harmonics of the firing frequency of the engine. At other harmonics the coherence was lower than 0.9, which would result in very little control.

While it was shown that the number of reference signals used during control was very important, the locations and type (microphone, tachometer or accelerometer signal) of the reference signals also affect the results. As illustrated in Table 5.2, in the case where three references were used, the total attenuation is as low as 6 dB when the accelerometers were located on the engine mount, up to 8.7 dB when one accelerometer was located on the oil fill stem and two on the firewall, inside the cabin. The peak reduction was also influenced by the position of the accelerometers, since reduction varied from 18.5 dB to 25 dB.

In conclusion achievable reduction was maximized when six reference signals were used (31 dB peak and 12 dB global), but using three well positioned reference signals provided adequate results, since all the harmonics were cancelled resulting in a flat frequency response at the error sensor. In the experiments presented in the next section, three reference signals were used. One accelerometer was positioned on the oil fill stem and two on the firewall (one on the side of the driver and one on the side of the passenger). It is also important to note that the performance of the actual control is determined by two other main factors. First, the system has to be causal, i.e. the reference must be 'upstream' and the detection of the disturbance must be such that the algorithm has enough time to compute the control signal to the actuators. Second, the number of reference signals influence the length of the filters used for the system identification and the control. The number of filters used in the system identification is the number of actuators multiplied by the number of error sensors. The number of filters used for

the control path is the number of actuators multiplied by the number of reference sensors. If more references are used, the number of filters is increased and therefore less coefficients can be used in each of the FIR filters. An alternative is to reduce the number of actuators and sensors used thereby reducing the number of filters needed for identification. Because the filters obtained with less coefficients are less accurate in modeling the paths of the controller (system identification and control), the attenuation obtained experimentally may be lower than predicted.

Table 5.2 Predicted reduction at the error sensor for different configurations of reference sensors.

configuration	**Peak attenuation (dB)**	**Total attenuation (40-500 Hz) (dB)**
1 Six references	31	12
2 Four References	29	9.7
3 Three References; optimized position	25	8.7
4 Three references on the firewall	18.5	8
5 Three references on the engine mount	24	6.2
6 Three references on the oil fill stem	23	6
7 One reference on the firewall	18	5.4
8 One reference on the oil fill stem	17	4.5

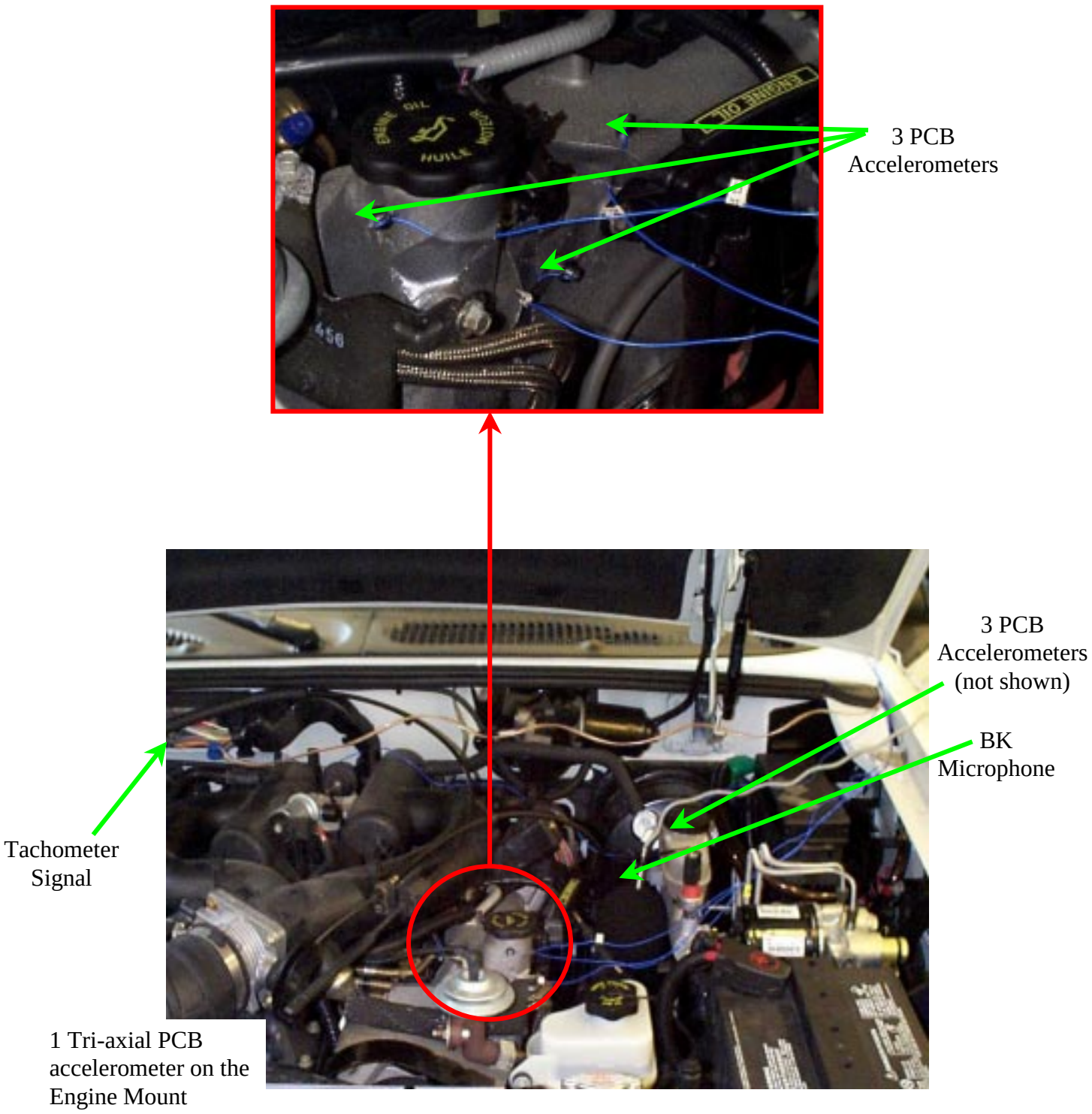

Figure 5.4 Location of the reference sensors in the engine compartment

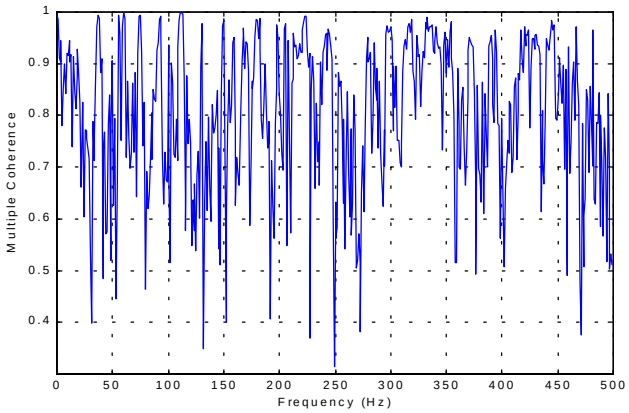

Figure 5.5: Multiple coherence with six reference signals

(Three on the oil fill stem and three on the fire wall floors)

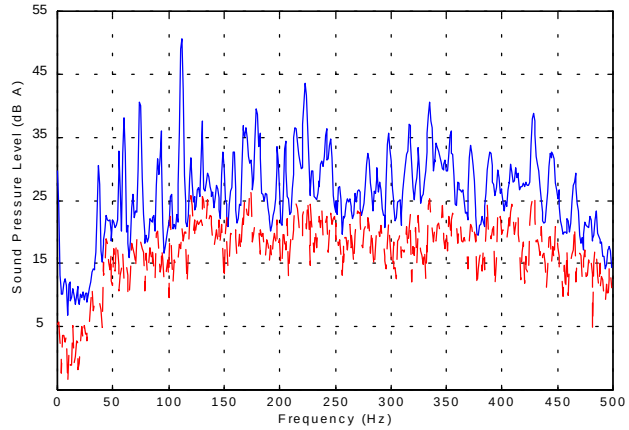

Figure 5.6 Sound pressure level at the error sensor - results with six reference signals

(Three on the oil fill stem and three on the fire wall floors)

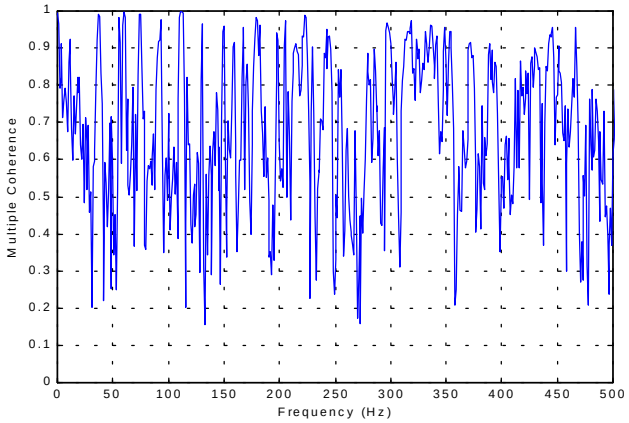

Figure 5.7 Multiple coherence with four reference signals

(Three on the firewall and one on the oil fill stem)

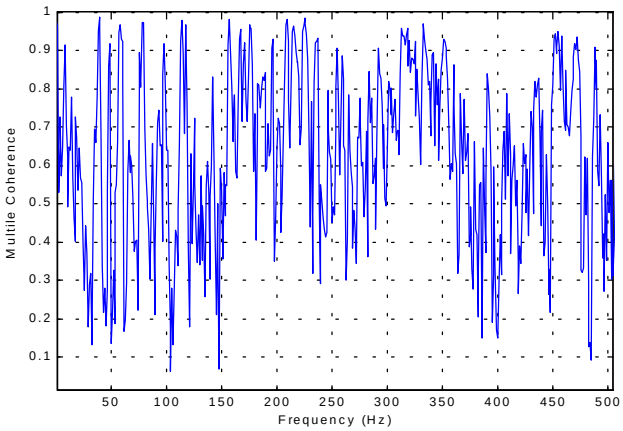

Figure 5.8 Multiple coherence with three reference signals

(Three on the firewall)

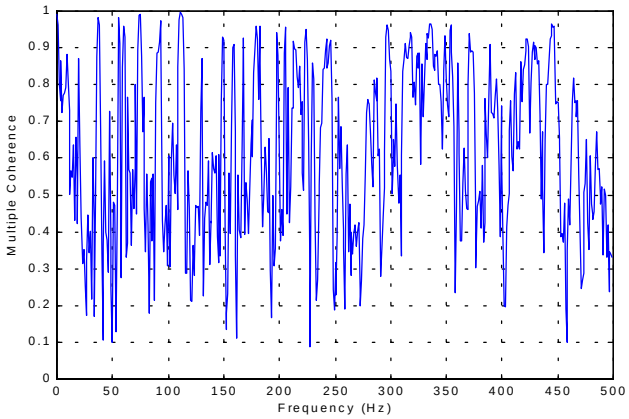

Figure 5.9 Multiple coherence with three reference signals

(Two on the firewall and one on the oil fill stem)

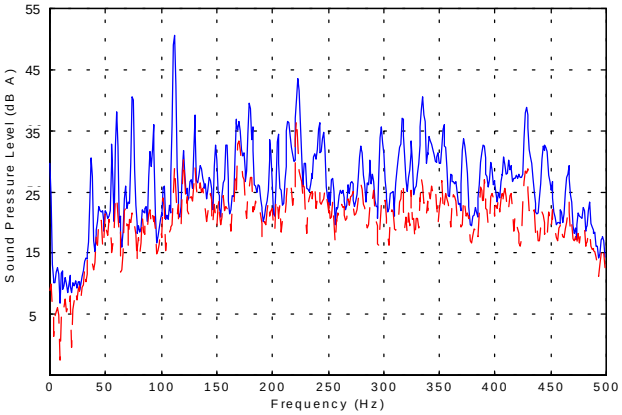

Figure 5.10 Sound pressure level at the error sensor - results with three reference signals

(Two on the firewall and one on the oil fill stem)

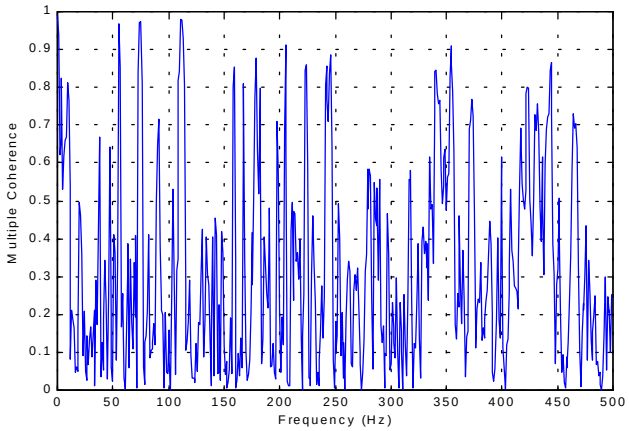

Figure 5.11 Coherence with one reference sensor
(One on the oil fill stem)

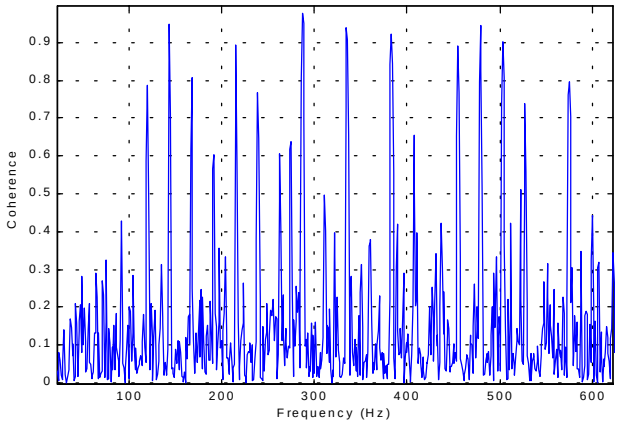

Figure 5.12 Coherence with one reference sensor
(Crank Pick-Up)

5.2.2 Experimental Procedure

The experimental set-up used to perform active control of the power train noise is described in Figures 5.13, 5.14 and 5.15. Figure 5.13 shows the different components of the system (microphones and speakers) in the interior cabin when control was performed with commercially available speakers. For the different configurations, the number of control sources and error sensors was varied. Three reference sensors were used for all the configurations, which involved two or four control actuators and two or four error sensors. Their locations are shown in the upper part of Figure 5.13. In the cases where two control sources were used, the control was

performed with the either speakers from the stereo system (left), or with the advanced piezoelectric speakers. In the cases where four control sources were necessary, two extra moveable speakers were added to the system. The moveable speakers have a 4-inch diameter diaphragm baffled in an enclosure, as shown in Figure 5.13. Their position is shown in the upper right corner of the figure. Also shown are the B&K microphones, which were used as error sensors. They were positioned at the height of the heads of the driver and passenger for all the configurations. A schematic showing the positions of the different components (error sensors and control sources) is shown in Figure 5.14. In the case two error sensors were used, each sensor was located at the location of the head of the passenger and driver. In the case four error sensors were used, the two extra microphones were positioned closer to the windshield.

Figure 5.15 gives more details concerning the signal processing of the data. Data were acquired at a sampling frequency of 2048 Hz, which is four times higher than the upper frequency of interest (500 Hz) and satisfies the Shannon criteria (the sampling frequency has to be at least 2.56 times the highest frequency of interest). 120 coefficients were used for the system identification because the impulse response of the system (dynamics of the path between each actuator and each error sensor) decays to zero. 150 coefficients were used for the filters of the control path, which was the maximum number that could be used with the settings described above. For both the system identification and the control path, Finite Impulse Response (FIR) filters were used to ensure stability. Figure 5.15 also shows that the signals from the reference and error sensors as well as the signals to the control sources, were amplified and band pass filtered between 40 and 500 Hz. Thus, the controller actually minimizes the sum of the pressure squared at the error sensors only between 40 and 500 Hz. As it will be shown later in Figure 5.16, the amplitude of the harmonics diminishes as the frequency increases. While their amplitude is as high as 30 dB over the engine background noise at frequencies lower than 300 Hz, they are only 5 dB above the background noise in the 300-450 Hz frequency band. The amplitude of the harmonics becomes negligible above 450 Hz. The signal was low pass filtered at 500 Hz because there is little energy in the signal at higher frequencies.

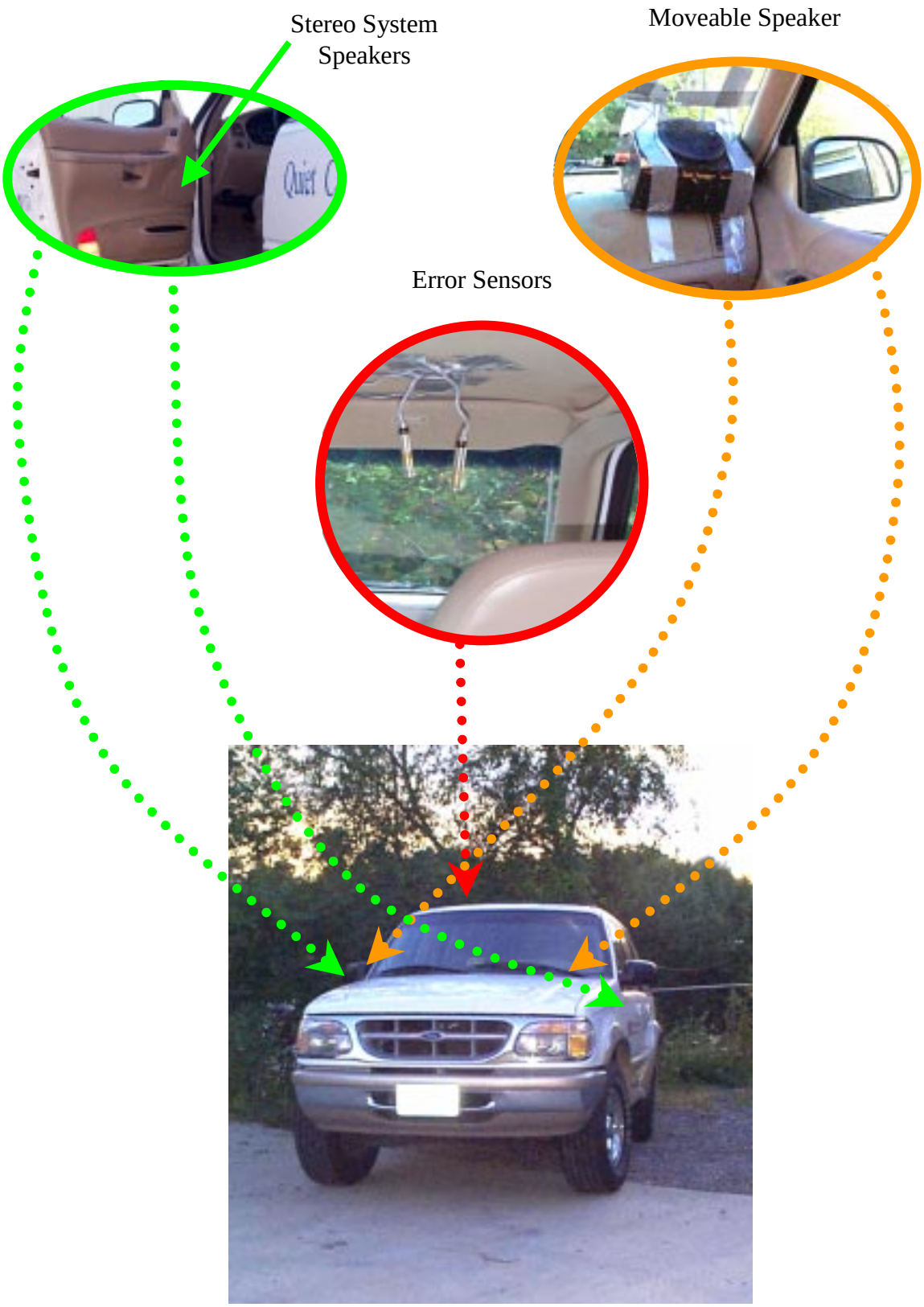

Figure 5.13 View of the automobile with actuators and sensors

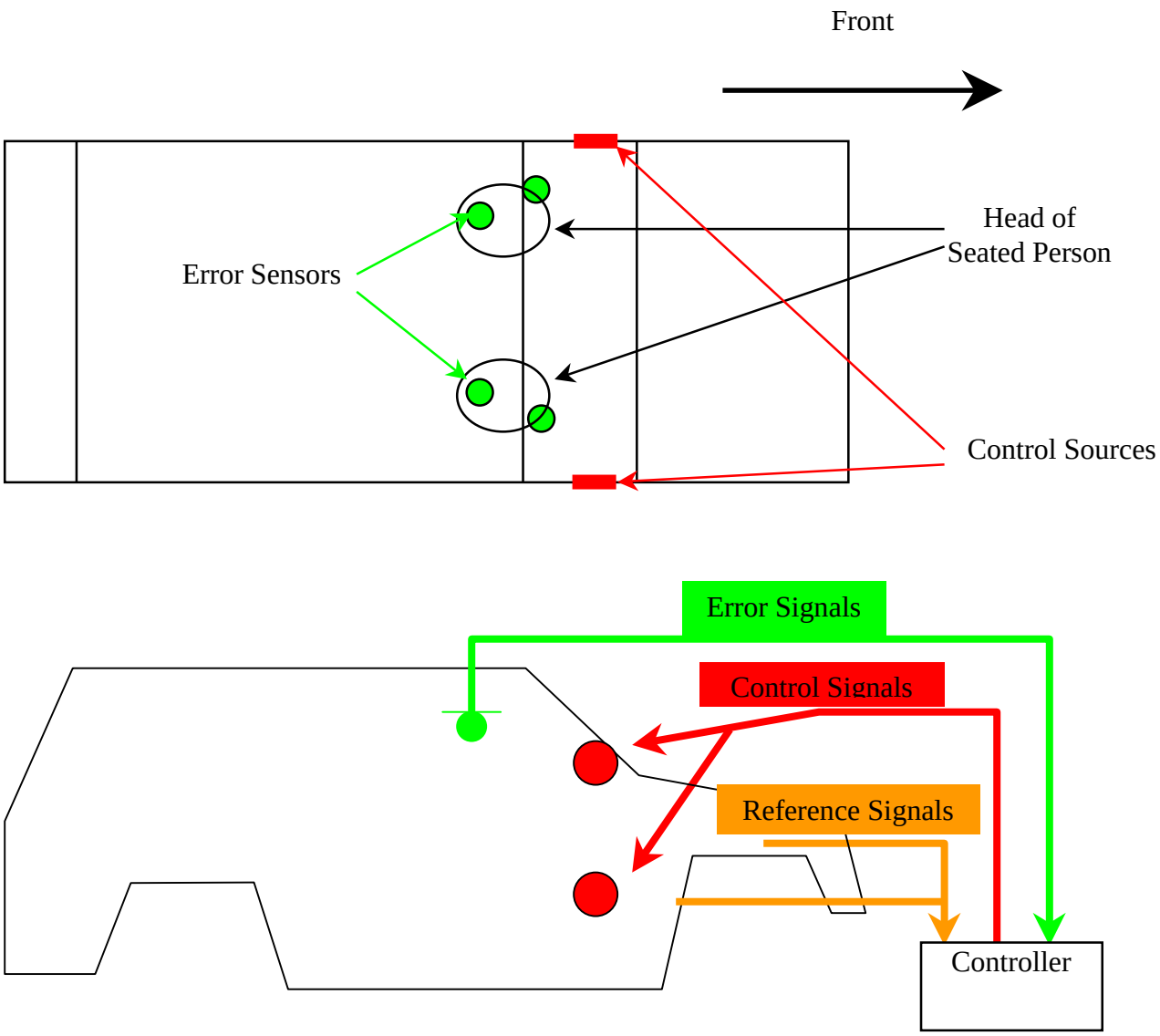

Figure 5.14 Schematic of the set-up showing the location of the error sensors and actuators

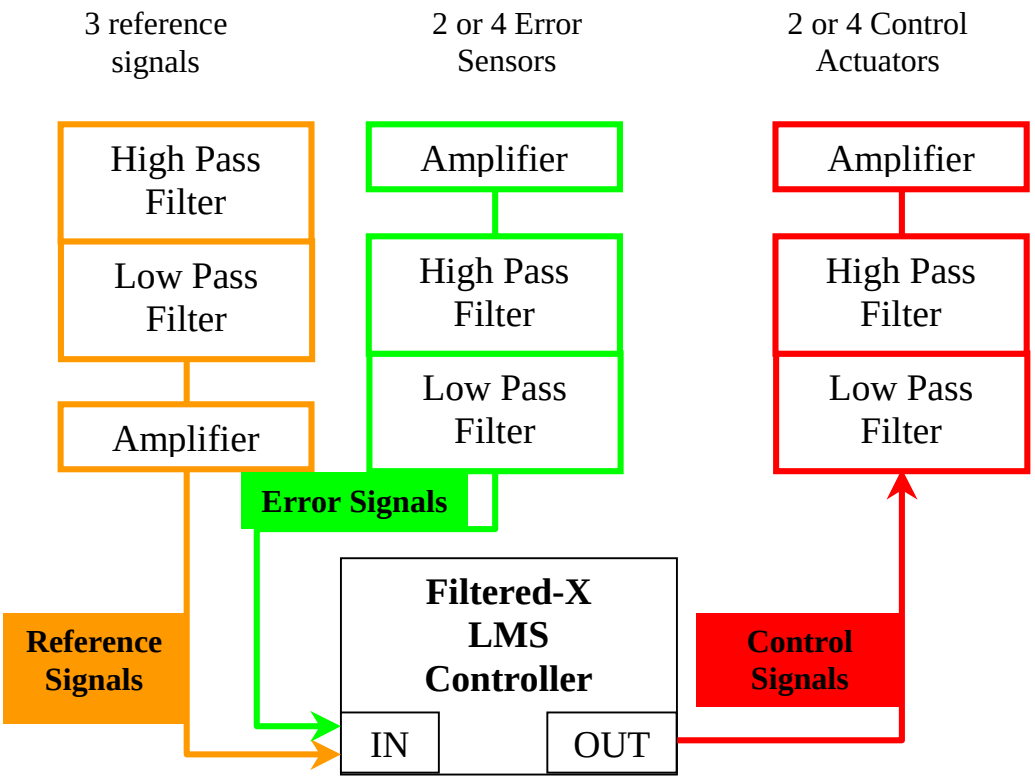

- Sampling Frequency: 2048 Hz
- No of coefficients for System Identification: 120
- No of coefficients for Control Signal: 150

Figure 5.15 Experimental set-up

5.2.3 Results Obtained in a Lab Environment

The frequency response function measured at the error sensor located at the head of the passenger before and after control is shown in Figure 5.16, in the case where two actuators and two error sensors were used. The error sensors were positioned symmetrically at the heads of the driver and passenger (Configuration number 2 in Table 5.3). One actuator was located in each front door as in Figure 5.13. The response is shown A-weighted between 40 and 500 Hz. The response is typical of what was measured at the error sensor. The signal before control is shown in a solid blue line. Note that from Figure 5.16. the response is highly dominated by the even harmonics of the firing frequency of the cylinders of the engine (the harmonics of the firing frequency that have the highest amplitude are shown with their frequency and number in parenthesis). For the case presented in Figure 5.16 the engine was turning at 2900 rpm, which corresponds to a fundamental frequency of 24Hz. The signal at the harmonics is up to 30 dB (144 Hz) higher than the background noise (20 dB A).

The response after control is shown in a solid red line. The effect of the control is to cancel most of the peaks that contribute most significantly to the response. The maximum peak reduction is 30 dB at 144 Hz. In fact, the harmonics are reduced to a level close to the background noise of the engine. Due to poor coherence between the reference signals and the error sensor, no reduction is obtained at 75 Hz. The poor coherence is due to the fact that this frequency is not a harmonic of the firing frequency of the cylinders. These results agree with the simulation, where a peak reduction of 30 dB and a global reduction of 8 dB had been predicted in the frequency range 40 to 500 Hz.

The global reduction in the frequency band of interest (40 to 500 Hz) is 7 dB. It is close to what was predicted by the simulation of section 5.2.1 (and illustrated in Figure 5.10) when three reference signals were used (8dB).

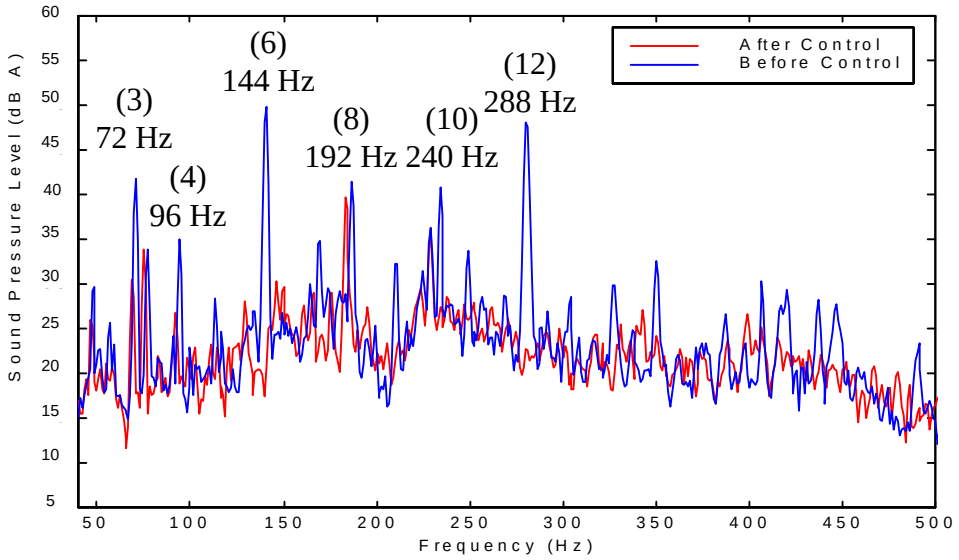

Figure 5.16 Sound pressure level at error sensor 2 in dB A

Table 5.3 presents the global reduction at the error sensors for different configurations of sensors and actuators. Four configurations are shown here, including three square systems, i.e., the number of actuators is the same as the number of error sensors (#1, 2 and 4). Systems 1 and 2 involve two actuators and two error sensors; system 4 involves four error sensors and four actuators. System 3 is an over-determined system (the number of error sensors is larger than the number of actuators) since two actuators are used with four error sensors.

The reduction obtained at the error sensors depends on the configuration. As was shown in chapter four, the reduction is larger for a square system than for an over-determined system. Table 5.3 shows reductions of approximately 6.5 dB for configurations 2 and 4, while only 2.5 to 4 dB for configuration 3. These results confirm those obtained in the test cavity as well as the theoretical prediction described in equation (2.9) (see section 2.1). Nevertheless, in configuration one, although the system is square (two actuators and two error sensors located on the driver's side), only a small reduction was obtained at the error sensors (3.3 and 3 dB).

Table 5.3 Attenuation at the error sensors (dB A) obtained with conventional speakers

#	Configuration	Error 1	Error 2	Error 3	Error 4
1	**2 by 2 (1)**	3.0	3.3		
2	**2 by 2 (2)**	6.4	6.4		
3	**2 by 4**	2.6	4.0	2.7	4.0
4	**4 by 4**	4.6	6.7	5.1	7.0

The reduction at the error sensors noted above is of great importance. Nevertheless, as was pointed out in section 2.1, poor sensor location results in large spatial spillover. In order to determine the effect that spillover may have on the results, the interior volume of the cabin was scanned to monitor the spatial distribution of the pressure before and after control. The scanning system is shown in Figure 5.17. Thirty PCB acousticel microphones were located in a horizontal plane. The microphones were positioned so as to form five lines of six microphones with a regular distance of four inches between each microphone. The horizontal plane was moved in the vertical direction as illustrated in Figure 5.17, and data were acquired for four vertical positions at both the driver's and the passenger's sides. The total volume scanned is a cube of 80 by 80 by 70 cm (H by W by L), which represents the volume occupied by the head and torso of a person normally seated in the automobile. In Figure 5.17 the system is positioned for scanning the volume occupied by the head and torso of the passenger.

In the next pages, results are presented for the four different configurations. In Figures 5.18, 5.19 and 5.20, part (a) shows the pressure distribution before control and part (b) shows the pressure after control. Figure 5.18 shows the results obtained with two error sensors for configurations 1 and 2. Part (c) shows the pressure after control for the second configuration of the error sensors. In Figures 5.19 and 5.20, part (c) shows the attenuation. Note from the figures that, before control, the sound pressure level is higher towards the boundaries of the cabin. There is a difference of 4 to 5 dB between the SPL at the boundaries and the SPL at the center of

the cabin. The distribution of the pressure results from the superposition of the acoustics modes of the cavity. As it was studied in the model of the test cavity in chapter 3, the nodal planes of the modes are perpendicular to at least one side of the cabin and are never on the boundary itself. Therefore, no linear combination of the modes can result in a distribution of the pressure with a minimum on the boundary. Because the boundaries of the automobile cabin are not as rigid as the boundaries of the test cavity, and because the damping is higher, the difference between maximum SPL and minimum SPL is not as high as it is for the test cavity (in chapter 4 (Figure 4.15 and 4.16) the difference was 10 dB). The pressure before control is not exactly the same in Figures 5.18 (a) to 5.20 (a), but the trends are the same. The difference comes from the experimental procedure. The volume was scanned and the pressure before control recorded for each configuration. Since the experiments were conducted on different days, the experimental conditions were not exactly the same. The temperature inside the cabin, and the engine speed have been slightly different. Since the difference was no more than 1 dB, it was ignored.

After control, for all configurations, a zone of quiet was created around the error sensors. The dimensions of this zone are different for all the configurations. Global control of the cabin was not achieved. As discussed in the introduction to this chapter, the damping associated with the acoustic modes of the cabin is high and global control of the pressure would require more actuators than the ones actually used.

In the first test, the two error sensors were located in the position of the driver, as shown in Figure 5.14. While a reduction of 3.3 dB was obtained in this position, spatial spillover of up to 4dB was recorded in the location of the passenger. This configuration is a good example of poor sensor placement because, first, the reduction at the error sensors is low and, second, spatial spillover occurs at a location where the head of the front passenger is located.

As illustrated in Figure 5.14, in the three other configurations the error sensors were located at both the driver and passenger positions. This positioning was chosen in order to avoid the spillover that occurred at the position of the passenger in the previous configuration. As a matter of fact, in these three cases reduction was obtained at both positions and spatial spillover occurred only in the corners of the scanned volume, where the head of the driver or passenger would not normally be while the car is in motion. The size of the zone of quiet created around the error microphones varies with the dimensions of the system. Although little difference in the

pressure profile was obtained between the 2 by 2 and 4 by 4 systems (Figures 5.18 (c) and 5.20 (b)), the configuration involving four speakers and four error sensors shows the best results.

These tests confirms what was pointed out in chapter four; as the number of speakers is increased, the number of degrees of freedom being controlled is higher and therefore the reduction is higher. Nevertheless, in the latter case, an increase of 6 dB occurred in one corner of the scanned zone, as shown in Figure 5.20 (c). In configuration 3 (Figure 5.19), very little spillover occurred. Figure 5.19 (c) shows only a 1 dB increase in the pressure in one corner of the volume. The tests also confirm the results of the experiments conducted on the test cavity in section 4.3. The reduction obtained at the error sensors is not as high as in configuration 4 (maximum 4 dB at the error sensors in configuration 3 and maximum 7 dB at the error sensors in configuration 4), but the reduction in the SPL is spatially more global.

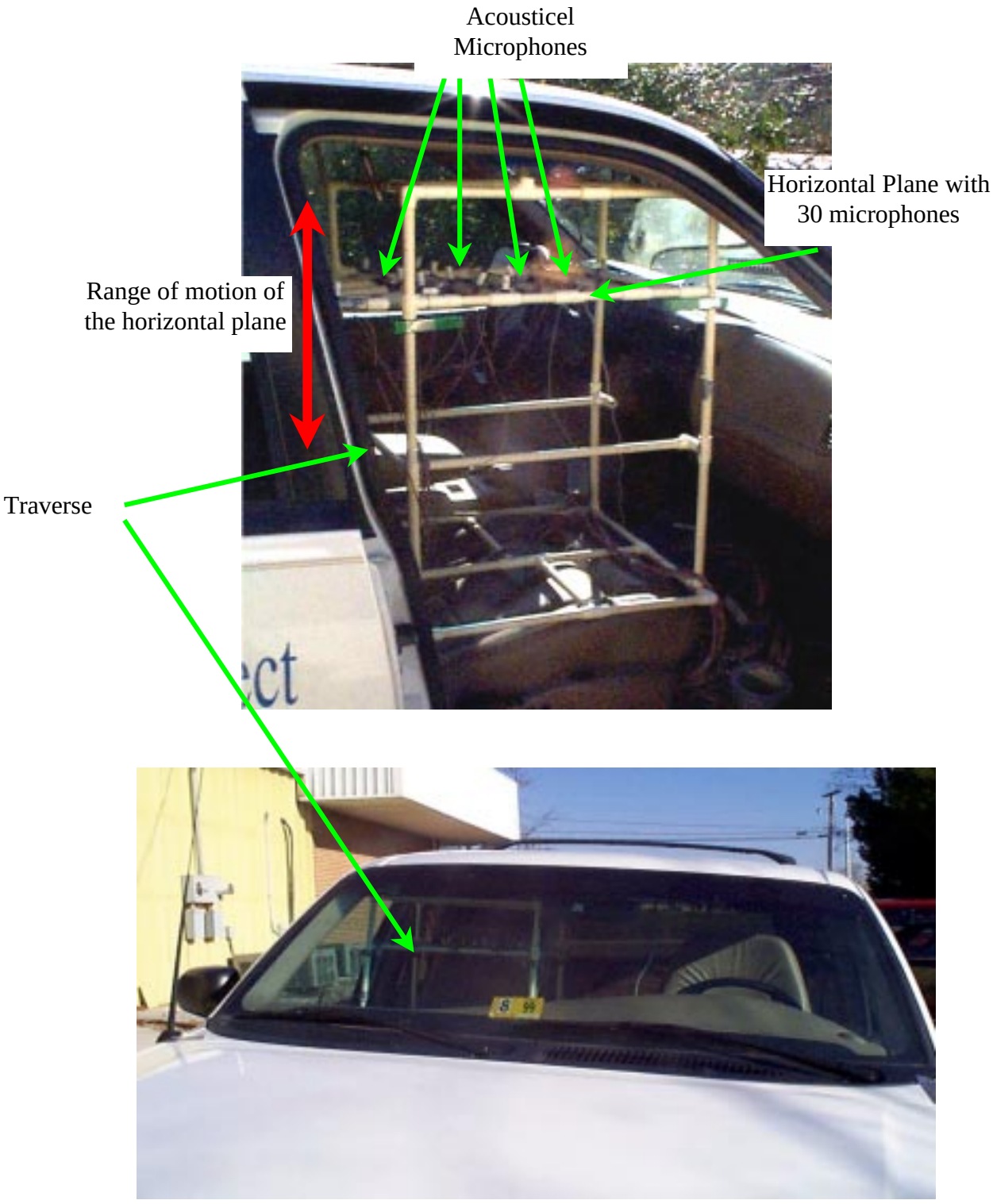

Figure 5.17 Scanning system

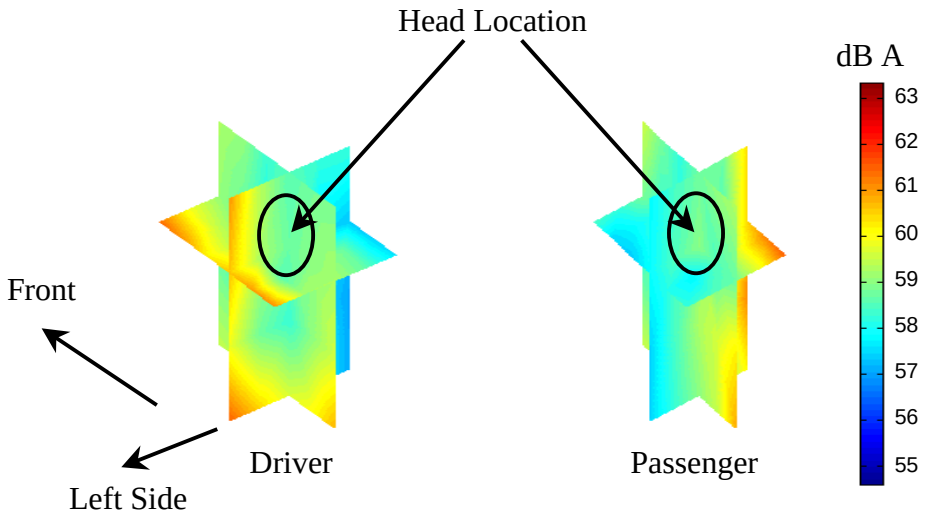

(a) Pressure before Control

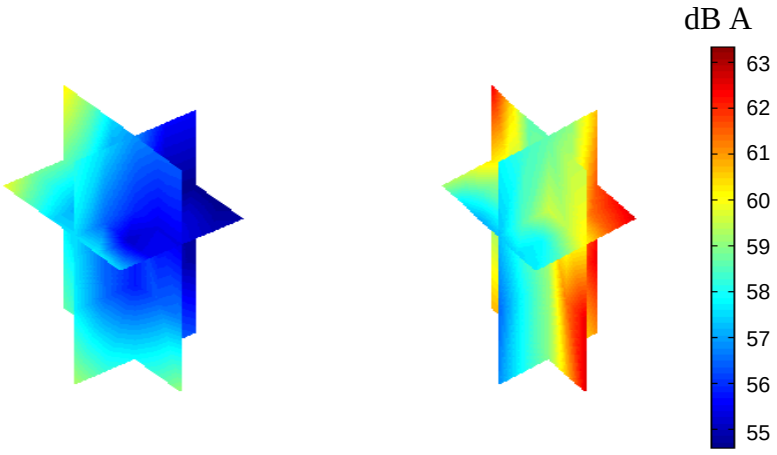

(b) Pressure after Control (configuration 1)

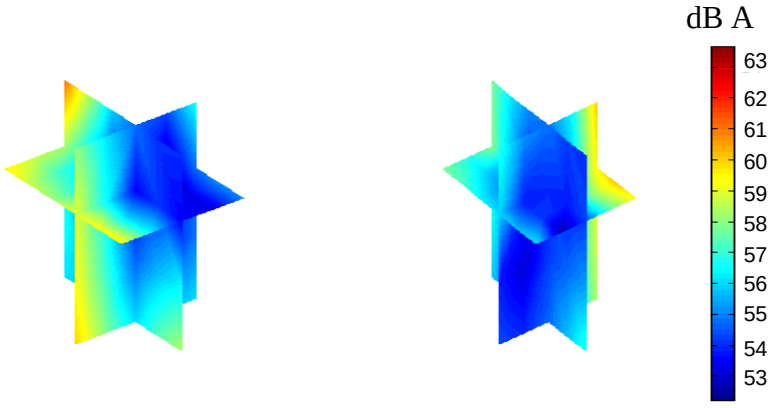

(c) Pressure after Control (configuration 2)

Figure 5.18 Spatial distribution of the pressure (2 by 2 systems)

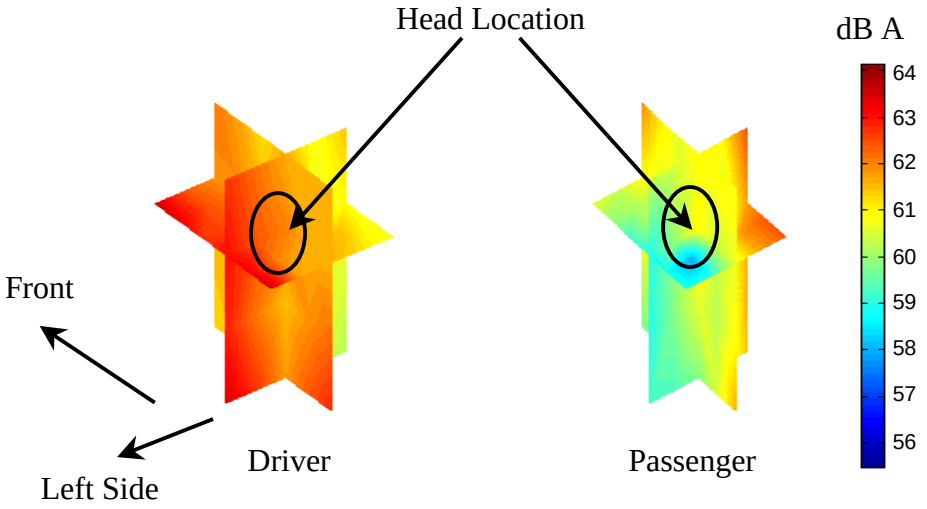

(a) Pressure before Control

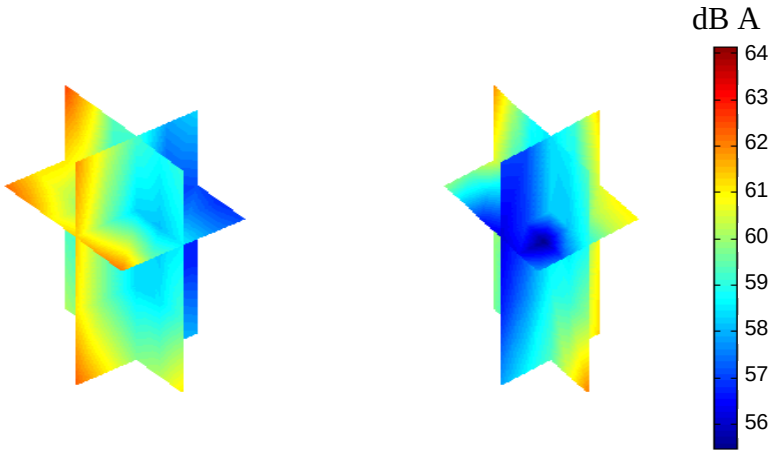

(b) Pressure after Control

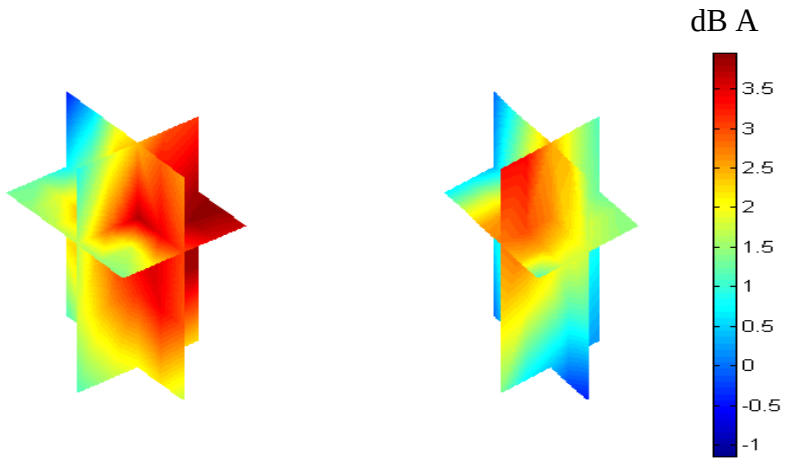

(c) Attenuation

Figure 5.19 Spatial distribution of the pressure (configuration 3)

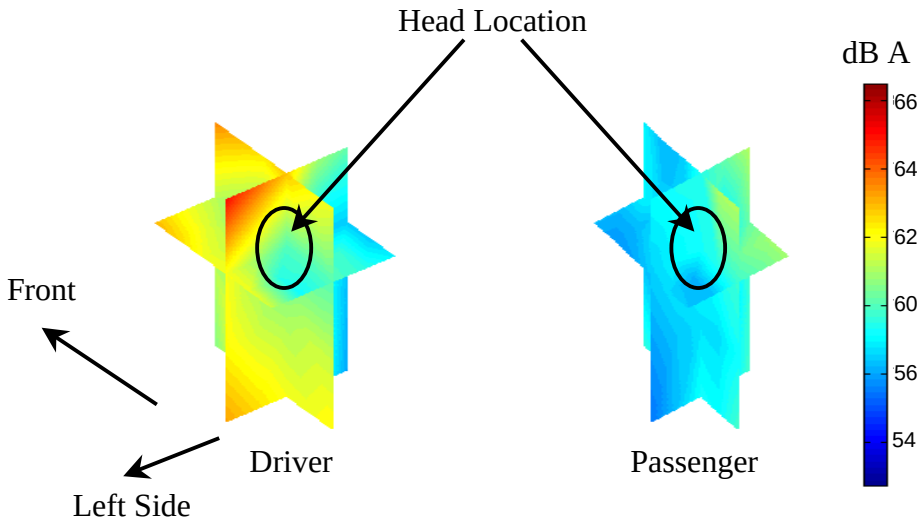

(a) Pressure before Control

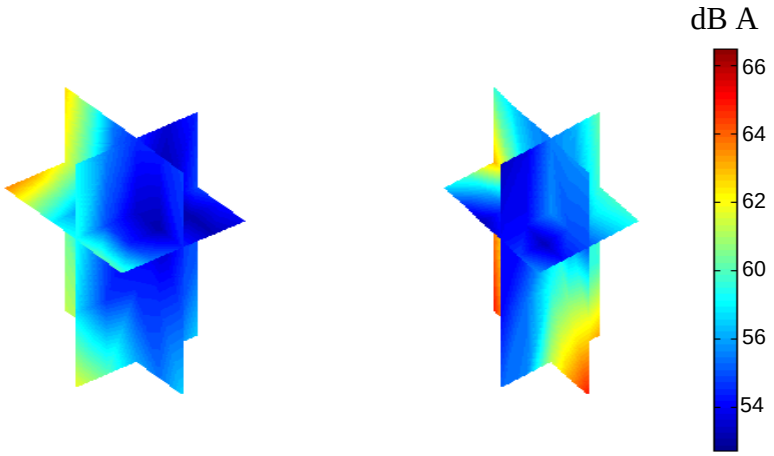

(b) Pressure after Control

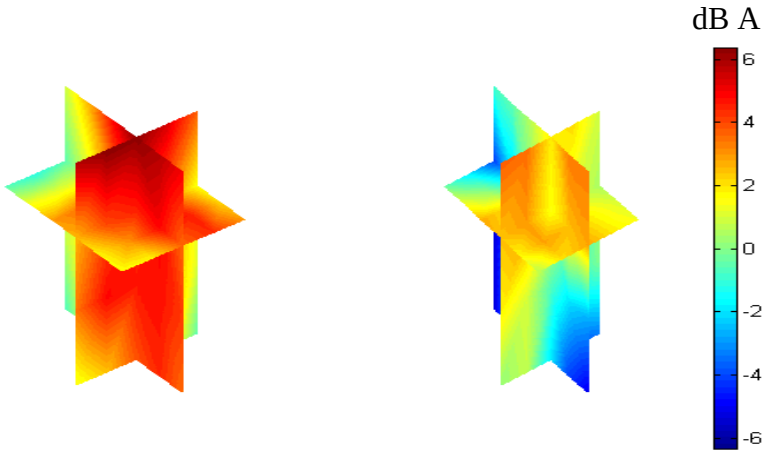

(c) Attenuation

Figure 5.20 Spatial distribution of the pressure (configuration 4)

5.2.4 Results obtained on the Road

The same experiment as the one performed in the laboratory environment was undertaken on the road. When the car is driven on the road, many sources of noise exist, typically due to the wind, due to the contact of the tires with the road and due to the power train. The car was driven on a steep road with a constant engine speed of 4300 rpm such that the power train noise dominates the other sources of noise. The experimental set-up was the same as before (Figures 5.13 to 5.15), but with the physical constraint of having all the equipment packed up in the trunk of the car. It must be pointed out here that conducting this experiment was not straightforward. Most of the equipment is not battery powered therefore it was necessary to connect a power inverter to the car battery in order to use the equipment. The volume occupied by the equipment was roughly two thirds of the volume of the trunk of the Ford Explorer. In order two avoid rattling noise due to the contact between each piece of equipment, each element was wrapped in foam. Such treatment also decreased the noise caused by the fans of the acquisition system, power inverter and PCs.

Experimental results are presented in Figures 5.21, 5.22 and Table 5.4 for a system involving two speakers and four error sensors, similar to configuration 3 of section 5.2.3. Figure 5.21 shows the frequency response before and after control. The response is very similar to the response obtained with the engine turning at 2900 rpm in the laboratory. The slight differences are due to the different load conditions. When the engine is turning in the laboratory, there is no load on the engine. During the road test, a constant load was applied to the engine because the car was driven at a constant speed on a road whose inclination did not change during the experiment.

The background noise of the engine is 30 dB A throughout the frequency band of interest (40 to 500 Hz), but the response is dominated by the harmonics of the firing frequency of the cylinders of the engine (36 Hz). The response at these frequencies is 10 to 25 dB above the background noise.

The response after control is shown in Figure 5.21 as a solid red line. The effect of the control is similar to the effect observed in the previous section. Maximum reduction of 20 dB is obtained at 432 Hz, and the response at the harmonics is decreased to a level close to the

background noise of the engine. In Figure 5.21, the harmonics are shown with their frequency and number in parenthesis.

The global reduction at the error sensors is given in Table 5.4. Once again, the results are very similar to those obtained in the laboratory, with overall reduction of 2.5 to 4 dB at the error sensors.

Table 5.4 Attenuation at the error sensors (dB A) obtained on a steep road

Configuration	Error 1	Error 2	Error 3	Error 4
2 by 4	4.1	2.5	3.5	3.4

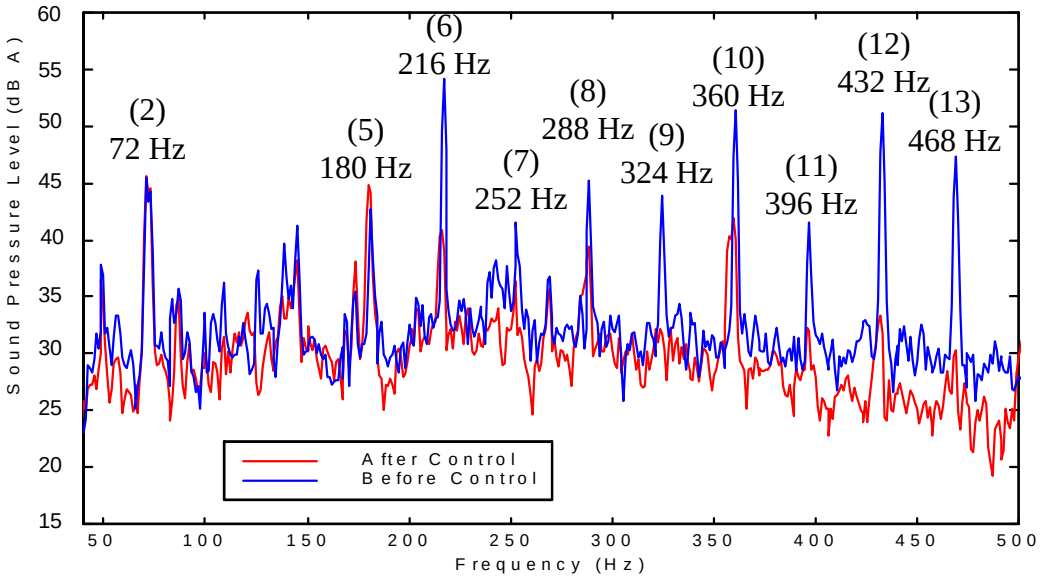

Figure 5.21 Sound pressure level (dB A) at error sensor 1

Regarding the scanning of the sound pressure level inside the cabin, for obvious technical and safety issues, the scan was performed only at the position of the passenger for three horizontal positions. The volume covered is therefore reduced to a cube of 80 by 80 by 50 (W by L by H). Results are presented in Figure 5.22 and show the pressure field before and after

control, together with the attenuation in the scanned volume. The zone of quiet obtained is similar in shape and size to the zone of quiet obtained with configuration 3 in the laboratory. Spatial spillover occurs in the corners of the scanned volume.

In conclusion, it was shown that results obtained on the road were similar to those obtained in the laboratory with the engine turning at a constant speed. The difference in frequency response at the error sensor are most likely caused by the difference in engine load conditions between the two experiments. However, the nature of the response is still the same (i.e., the response is dominated by the response at the harmonics of the cylinder firing frequency). In the case when the automobile was driven on the road, the higher frequency peaks contribute more to the global response than in the case where the car was in the laboratory. In terms of spatial distribution of the pressure before and after control, as well as the attenuation at the error sensors, the results are very similar. They show that a system to actively control power train noise can be designed in a laboratory environment, with the engine turning at a constant speed. As noted before, the engine load conditions were different when the car was driven on the road, resulting in a modification of the frequency response measured at the error sensors. The controller performed well, since all the harmonics of the firing frequency of the engine were cancelled and a zone of quiet was created around the head of the passenger. Nevertheless, it must be pointed out that the amplitude of the harmonics did not decrease as the frequency increased, as was the case when the car was in the laboratory (see Figure 5.16). In terms of global reduction at the error sensors, better results may be obtained if the signal is low pass filtered at a higher frequency. However, this system might not be practically feasible since the sampling frequency of the controller would be higher in this case, more coefficients should be used in the filters (because the frequency content is wider and therefore an accurate FIR filter model requires more coefficients).

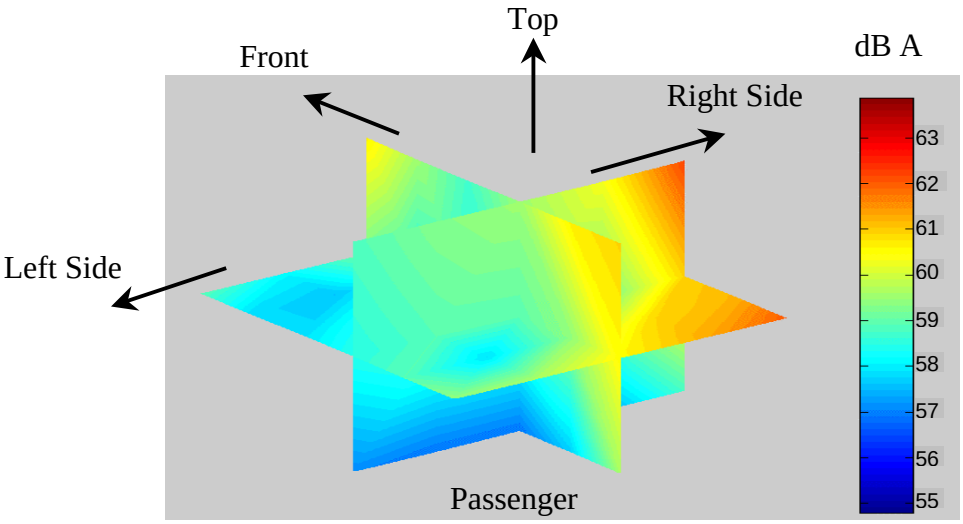

(a) Before Control

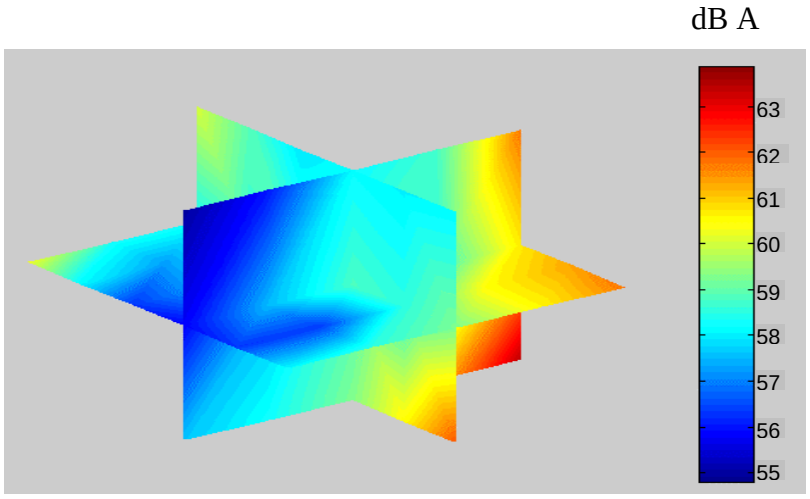

(b) After Control

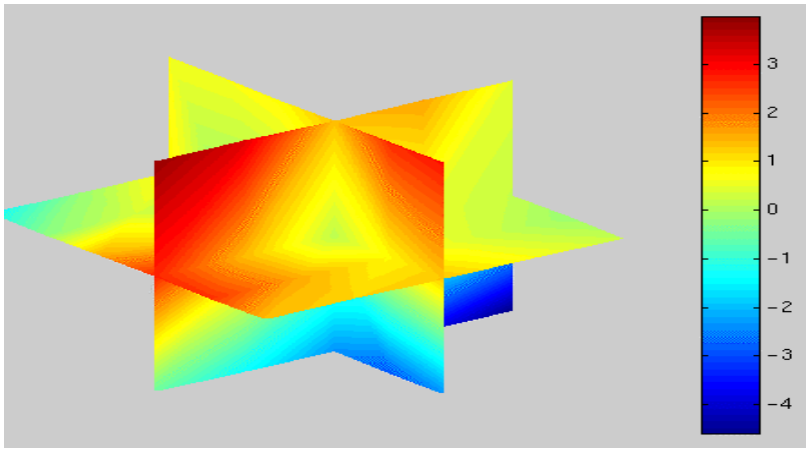

(c) Attenuation

Figure 5.22 Spatial distribution of the pressure – results obtained on the road

5.2.5 Control using Advanced Piezoelectric Speakers

This section covers results of active control of power train noise, with the same reference signals as used in the previous sections, but using piezoelectric compact speakers. Material system Inc., Penn. State University and Virginia Tech have developed these speakers [55]. They are presented in appendix B. The configurations used during the test involving conventional speakers were no longer suitable because only two piezoelectric speakers could be built (only six double amplifier drivers were provided by the team members of Material system Inc. and Penn. State University). As discussed in Appendix B an C, the output of the source is low at frequencies below 150 Hz, Therefore, the control was performed in a reduced frequency band. The frequency band in which the control was performed is 150 to 500 Hz. Three different configurations of actuators and sensors were tested. One configuration used one actuator was used with one error sensor. The actuator was located in the door as illustrated in Figure 5.23. The source was maintained in position by the arm rest and is fixed to the door with two straps of duct tape. The source was located on the passenger door, while the error sensor was located at where the head of the passenger would be. The two other configurations involved two sources, which where positioned in both front doors shown in Figure 5.23. The second configuration used two error sensors positioned at the head location of the driver and the passenger as in sections 5.2.2 and 5.2.3. In the third configuration, four error sensors were used and located at positions similar to those used in configuration four of section 5.3.3.

The results are presented in Figure 5.24 and Table 5.5. Figure 5.24 shows the response at microphone one for the case where the sound field is controlled using two error sensors and two sources. As it has been pointed out before, the solid blue line, which shows the sound pressure level before control, is highly dominated by the response at the harmonics of the firing frequency of the cylinders. In this particular case, the engine was turning at 3200 rpm. The solid red line shows the response after control. Similarly to what was observed previously, the response after control at the harmonics is reduced to level close to the background noise of the engine. Reduction of 18 dB was obtained at 159 Hz, so that the response after control at this frequency is 6 dB above the background noise. Even though the attenuation is lower at other frequencies, for instance 14 dB at 291 Hz, the response after control is completely reduced into the background noise. Similar results are obtained at the highest harmonics.

Table 5.5 shows the global attenuation computed in the 150 to 500 Hz frequency band at the error sensors for the three different configurations. In the configuration involving one secondary source and one error sensor, the attenuation is 3.9 dB at the error sensor. When the number of secondary sources is increased, the reduction obtained at the error sensors increases also. In the configuration with two sources and two error microphones reduction of 6.9 dB was achieved at error sensor one. This is similar to the control achieved with the conventional speakers from the stereo system. These results suggest that the reduction at the error sensor depends on the number of secondary sources. This is also true for fully determined systems (i.e. the same number of actuators and sensors are used). When the system is over-determined, which is the case of the third configuration (two sources and four error sensors), the reduction at each error sensor is lower than in the case of a fully determined system with the same number of actuators. This result agrees with those presented in section 5.3.2 and chapter four, where it was also seen that the control was more global, in terms of spatial distribution, for over-determined configurations.

The experiments presented in this section demonstrate that the piezoelectric sources can be used to control power train noise above 150 Hz. Under 150 Hz, control is not possible. Three solutions are recommended. First, these sources have to be better manufactured in order to solve the rattling noise problem. Once the rattling problem is solved, the sources can be driven with a higher voltage, where the sources radiate more sound making control at frequencies under 150 Hz possible. Second, a larger diaphragm can be so that less displacement is required to radiate a given pressure level in the automobile. Third, a new driver can be developed to generate higher displacement of the diaphragm at low frequencies.

Figure 5.23 Location of the piezoelectric actuator

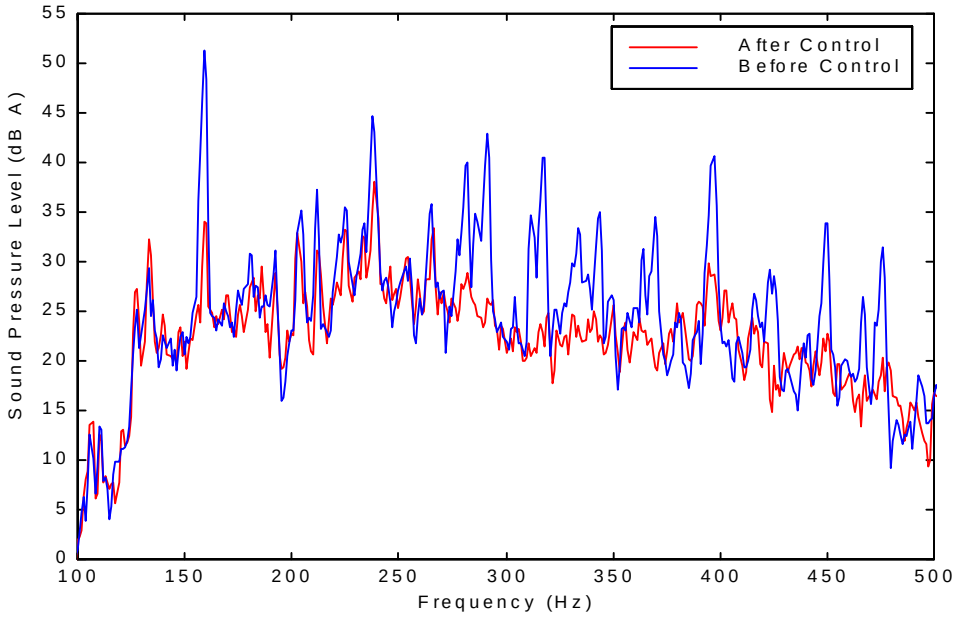

Figure 5.24 Sound pressure level (dB A) at error sensor 1 (2 by 2 system)

Table 5.5 Attenuation at the error sensors (dB A) obtained with piezoelectric actuators

Configuration	Error 1	Error 2	Error 3	Error 4
1 by 1	3.9			
2 by 2	6.9	4.3		
2 by 4	2.4	4.8	1.7	3.8

5.2.6 Conclusions

It has been shown that application of active control of power train noise in the interior cabin of a Ford Explorer yields good results. First, tests demonstrated that attenuation of up to seven decibel over a large frequency band (40 to 500 Hz) was achievable at the error sensors. Best results were obtained with a system involving three reference accelerometers, four conventional speakers used as control sources, and four error sensors located at the head level inside the cabin of the vehicle. The response at the error sensors before control was strongly dominated by the

response at the harmonics of the firing frequency of the cylinders. During the tests, the fundamental frequency was 24 Hz when the engine was turning at 2900 rpm, and 36 Hz when the car was driven on a steep road. The effect of the control was to reduce the amplitude of the peaks (maximum of 30-dB attenuation) at these frequencies. The response after control was flatter, and it was possible to lower the response at the harmonics close to the background level noise of the engine. Due to the very high damping inside the cabin of the automobile, there are a lot of modes that contribute to the response. Thus, in order to obtain global control of the pressure field, more control speakers would be required.

In terms of spatial effect, spillover appeared only in the corners of the volume scanned (head and torso of passenger and driver), at positions where the head would not be positioned during normal use of the vehicle. In fact, a large zone of quiet was created around the error sensors (i.e. around the head of the driver and passenger). The extent of the zone of quiet was increased as the number of error sensors and actuators was increased. The largest zone of quiet had the shape of a sphere centered at the error sensors (i.e., head of the driver and passenger). The diameter of the sphere was approximately 60 cm when four error sensors and four control sources were used.

A test performed while the car was driven on a steep road showed results similar to those obtained in the laboratory. The response at the error sensors before and after control, and the spatial distribution of the sound pressure in the cabin showed the same trends as those obtained in the laboratory. This implies that tests performed in a laboratory environment with the engine turning at the desired speed can be used to design an active noise control system for power train noise of a vehicle being operated on the road.

In the last section, prototype compact lightweight piezoelectric speakers were implemented as control sources. The results obtained with these speakers were comparable to those obtained with commercially available speakers. Nevertheless, the pressure response of these sources at very low frequencies (below 150 Hz) was too low to cancel the first harmonics of the signal. If the first harmonic were not filtered, the overall noise reduction would be decreased. In the case of configuration 2, the reduction at error sensor 2 was estimated to be 4.6 dB, instead of 6.9 dB if the first harmonic is not filtered. It was estimated that these tests demonstrated the potential of lightweight and compact sources to cancel power train noise in the Ford Explorer.

5.3 Active Control of Road Noise

The noise caused by the interaction of the tires with the road surface is also of great concern for the acoustic comfort of automobile passengers. As discussed in section 5.2.3, power train noise is predominant when the car is driven on at steep road. When the car is driven at a normal steady speed on a rough road, the interaction of the tires with the road is the principal source of noise in the cabin. This section covers the work performed for active control of road noise inside the cabin of the Ford Explorer. As it will be shown throughout this section, the problem of active road noise control is much more challenging than the problem of active control of power train noise. There are two main reasons for the complexity of the problem. First, the number of uncorrelated sources, which contribute to the acoustic response inside the cabin is large and difficult to identify. Second, the response at the error sensor is broadband in nature, and is not dominated by the response at a few harmonics as is the case for power train noise.

A discussion on the selection of reference signals necessary for the feedforward control approach (see section 2.3) is presented in section 5.3.1. It includes principal component analysis as well as the analysis presented in section 5.1 for reference signal selection. Section 5.3.2 covers the results obtained when the car was mounted on a dynamometer. In this particular case, the front wheels of the automobile were driven at a constant speed of 53 mph by a 20-cm-radius drum. The limitations of this test and the results will be discussed. In section 5.3.3, tests performed at Goodyear in Akron, Ohio, will be discussed. During these tests, the left front wheel of the car was driven at a constant speed by a 10-feet-diameter drum. The tests described in sections 5.3.2 and 5.3.3 are fairly different because the drums that are driving the front wheels have different characteristics. In the last section, preliminary results of control performed on a rough road will be shown.

5.3.1 Reference Signals Selection

Previous work on active control of road noise [29] showed that the number of reference signals is of paramount importance in controlling noise resulting from the interaction of the tires with the road surface. The structural-acoustic system is much more complicated in this case than in the

case of controlling power train noise. The four wheels are clearly identified as four independent sources of vibration. These vibrations travel through the body of the car and thus generate noise in the cabin. There are also acoustic paths through which the noise generated by the contact of the tires with the road surface travels. These paths go through via the air surrounding the cabin and through the body of the car into the cabin.

Two complementary methods are presented in the next two parts for the selection of the location of the reference transducers necessary for the feedforward control approach. In a first part, a principal component analysis was performed to determine the number of independent noise sources present when the car was driven on a coarse road. This method does not provide information concerning reference signal locations; therefore in a second part, the analysis presented in section 5.1 was applied to the problem of road noise to optimize the locations of the reference transducers.

a. Principal Component Analysis

Principal component analysis [37] has been previously used in active noise control work as a method to identify the number of independent disturbances [29]. While this method does not provide any insight into the best reference sensor locations, it is useful in determining the number of reference signals required to perform active noise control, since in general the number of references has to exceed the number of independent sources [29]. In order to perform this analysis, six accelerometers were positioned on the body of the car as in Figure 5.25. The car was driven on a coarse road in order to obtain road noise inside the cabin. The time history of the signals from the accelerometers were recorded at a sampling frequency of 4096 Hz and the anti-aliasing filters were set to 1000 Hz.

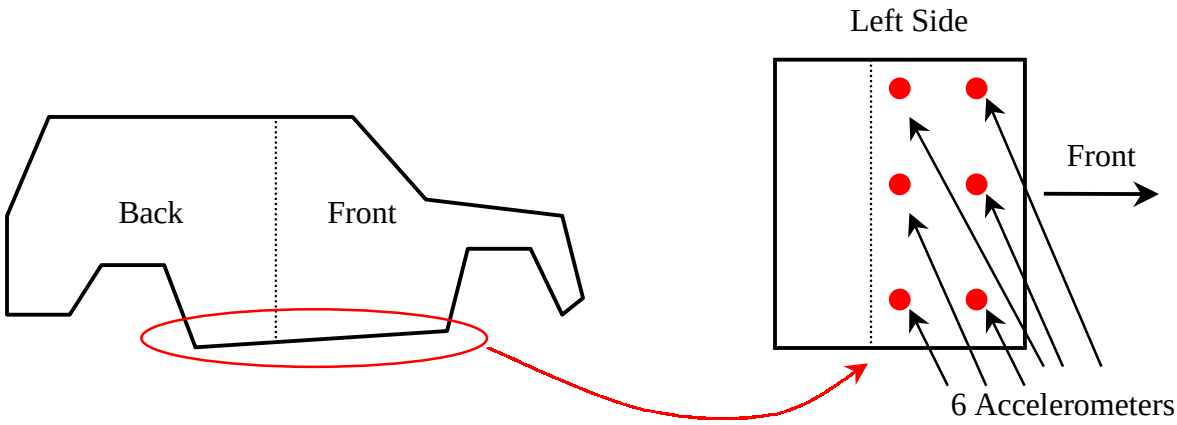

Figure 5.25 Schematic showing the positions of the accelerometers

For all the signals, the auto-spectrum (G_{xx}), as well as the cross-spectrum (G_{xy}) were computed to form the matrix G (f):

$$G(f)=\begin{bmatrix} G_{11}(f) & G_{12}(f) & \dots & G_{16}(f) \\ G_{21}(f) & G_{22}(f) & \dots & G_{26}(f) \\ & \dots & & \\ G_{61}(f) & G_{62}(f) & \dots & G_{66}(f) \end{bmatrix}. \qquad (5.4)$$

After singular value decomposition [29, 37], the G matrix can be written in the form:

$$G(f)=U(f)\Lambda(f)U^{H}(f), \qquad (5.5)$$

where Λ(f) is a diagonal matrix containing the singular values. The singular values can be considered as being the cross-spectrum density matrix of a set of uncorrelated virtual signals. The relationship between the virtual signals and the real signal is given by U [29]. The number of significant singular values at each frequency is thus the number of significant sources at that frequency.

The singular values of the matrix G are shown in Figure 5.26 between 40 and 1000 Hz. The Figure shows that while three components dominated above 500 Hz) no component really dominated at lower frequencies (40 to 200 Hz). At 200 Hz, six singular values are within 25 dB.

At 100 Hz, the six singular values are within 35 dB. This means that the number of significant independent sources of vibration is higher than six in the frequency band of interest. As it has been pointed out in [29], in order to obtain satisfactory results with a filtered-X feedforward LMS control, the number of reference signals has to exceed the number of independent sources. Therefore, for the case presented here, it can be concluded than more that seven reference signals are required to obtain significant results at frequencies as low as 200 Hz. The presently VAL available controller has only four input channels for reference signals. This implies than only small control is achievable at frequencies below 500 Hz with the present 1998 version VAL controller.

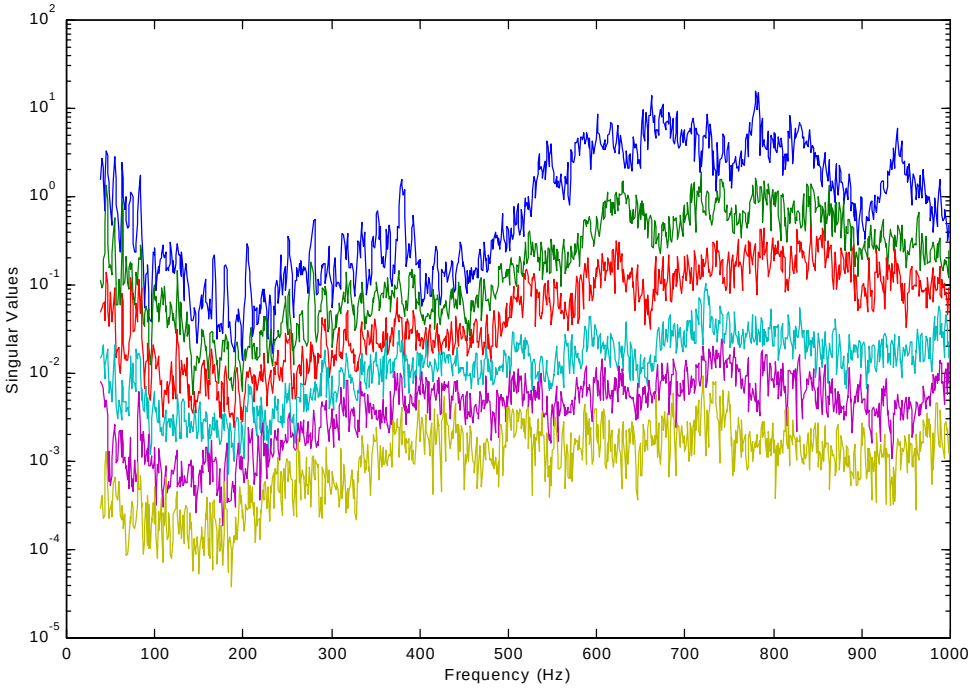

Figure 5.26 Singular values

b. Optimization of the location of the reference sensors

This section covers simulations based on the method presented in section 5.1. Using equations (5.1) and (5.3) the remaining noise after control can be estimated. Candidate accelerometers have been located on the wheels (see Figure 5.27), the body of the car (see Figure 5.25), the suspensions, as well as on the firewall at locations similar to those used for power train noise control. Signal acquisition from the error sensor located at the head of the passenger and from the reference accelerometers was performed using the same experimental set up as before (Figure 5.3). The multiple coherence function, together with the estimation of the noise after control, have been computed for several configurations of reference sensors. Although the hardware used during the actual control experiments had only four input channels for reference signals, the multiple coherence using eight, six and four accelerometers were computed to further investigate the influence of the number of reference signals on the performance of the control algorithm.

Results are presented in Table 5.6. They confirm the conclusion reached for the principal component analysis, i.e., that more than six references were required to achieve substantial control in a wide frequency band. When eight references were used, a reduction of 11.7 dB was achieved in a frequency band from 40 to 400 Hz. The reduction was also computed in a narrower frequency band. Reduction of 14 dB between 100 and 200 Hz. The coherence was above 0.9 for most of the frequency range of 40 to 500 Hz. This indicates that the control should be very good at all frequencies. As the number of references was decreased, the achievable reduction also decreased. While reduction of 9dB between 100 and 200 Hz was achieved with six reference sensors, only a 7-dB reduction was achieved with four references in the same frequency band. Table 5.6 also shows results for two configurations of four reference sensors. In configuration 1, three reference sensors where located on the front right wheel and in three perpendicular directions as shown in Figure 5.27, as well as on the firewall in the left side of the cabin. This configuration was chosen for control at an error sensor located at the head level of the passenger. It is assumed that most of the energy of the signal is coming from the vibration of the front right wheel and that little contribution comes from the left wheel. In configuration 2, one accelerometer was located on the suspension arm of each front wheel as well as on the body

of the car where the suspension arms connect with the body. These two configurations showed little difference in terms of noise reduction at the error sensor. In previous work, six error sensors were typically used and positioned as shown in Figure 5.27 for experimental active control of road noise. In this section, the simulations showed that as expected the attenuation is not as good when using four reference sensors instead of six. However, the but difference is small (2dB).

In conclusion, when four reference signals were used, significant reduction was achievable in a narrow frequency band (between 100 and 200 Hz). Unless eight references were used, very little control was achievable on a larger band (between 40 and 400 Hz). These results agree with those obtained during the principal component analysis. Nevertheless, because of hardware limitations, the experiments presented in the next three sections, use only four reference sensors positioned as in configuration one for control.

Table 5.6 Reduction at the error sensor; simulation for road noise

Configuration	**Attenuation 40-500 Hz**	**Attenuation 100-200 Hz**
4 references (configuration #1)	5.2	6.9
4 references (configuration #2)	5.5	7.1
6 references (3 on each front wheel; Figure 5.29)	7.8	8.8
8 references (3 on each front wheel, 2 on firewall)	11.7	14.2

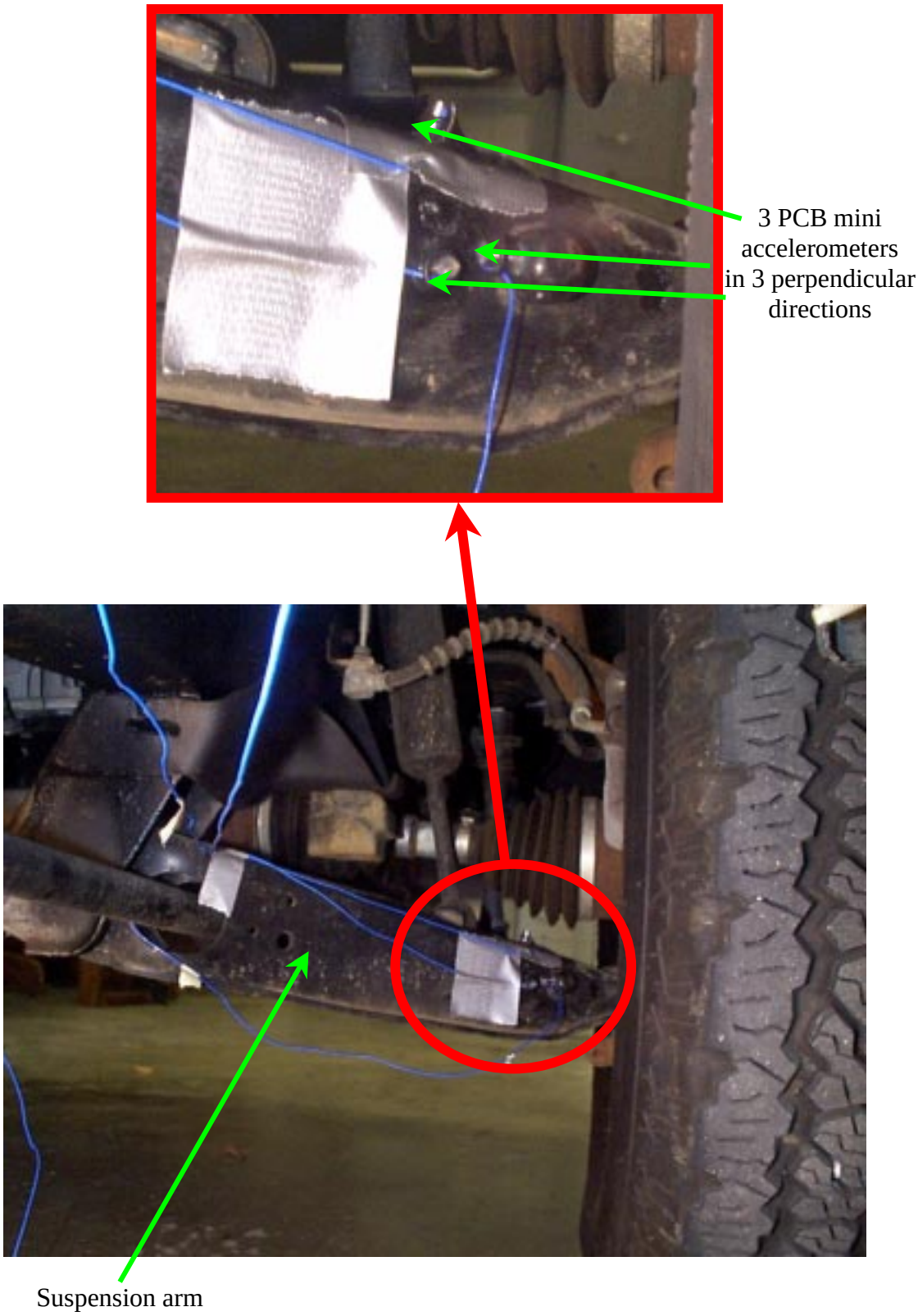

Figure 5.27 Location of the accelerometers on the wheel

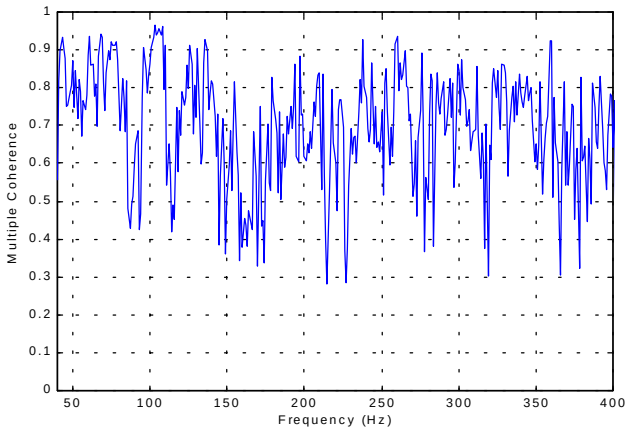

(a) Multiple Coherence; Configuration #1

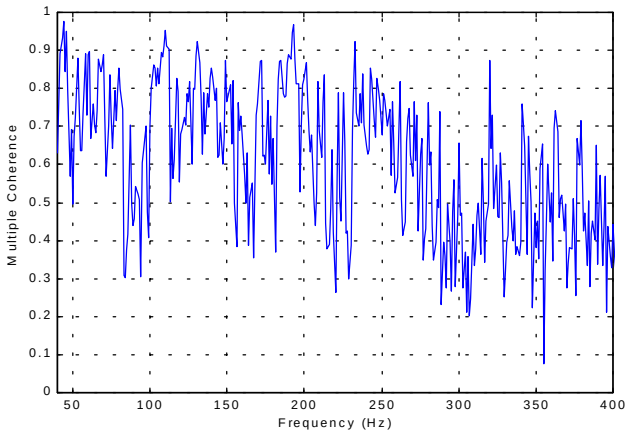

(b) Multiple Coherence; Configuration #2

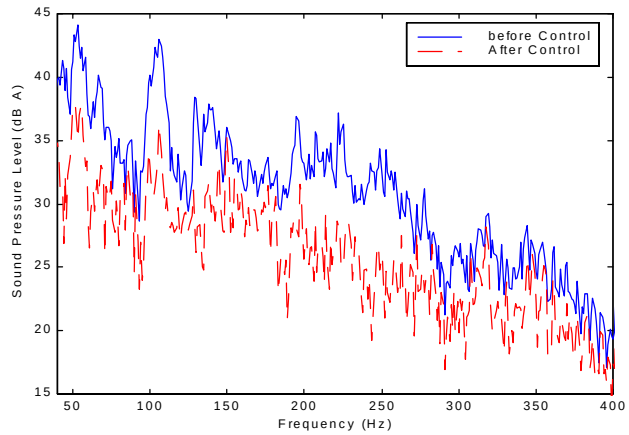

(c) Achievable Control; Configuration #2

Figure 5.28 Results with four reference sensors

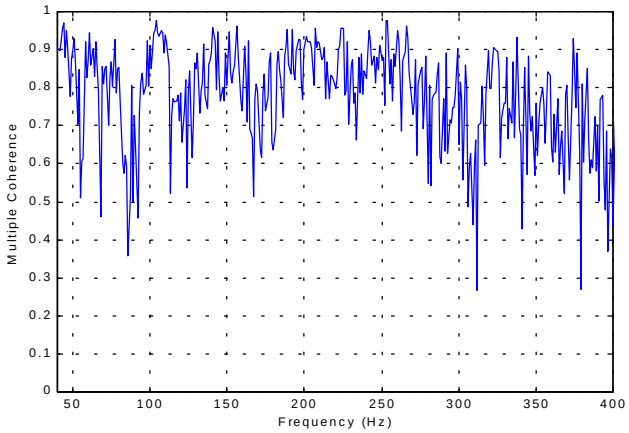

(a) Multiple Coherence

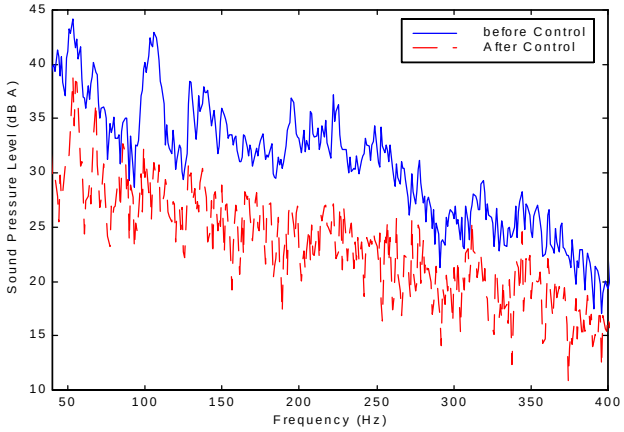

(b) Achievable Control

Figure 5.29 Results with six reference sensors (three on each front wheel)

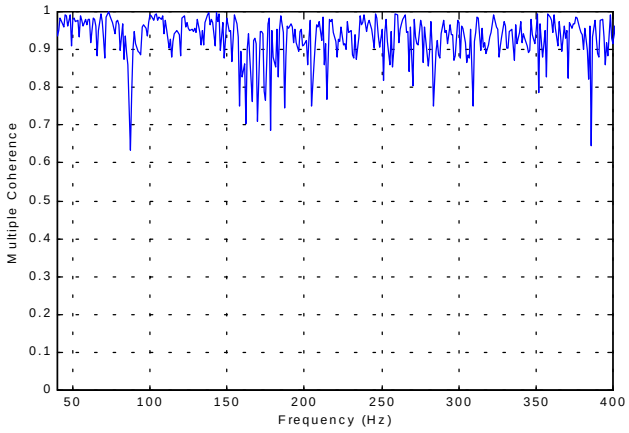

Figure 5.30 Results with eight reference sensors, three on each front wheel and two on each side of the firewall

5.3.2 Results obtained on a dynamometer

This section covers an experiment performed at Volvo Trucks in Dublin, Virginia. During this test the front wheels of the car were mounted on a dynamometer (with a smooth roller surface) to simulate a 53mph drive, as illustrated in Figure 5.32. The automobile is in neutral with the engine off while the dynamometer is running. Under these conditions, the only source is due to the contact of the front tires with the roller of the dynamometer. Several tests were performed involving four reference sensors and different configurations of actuators and sensors. Three reference accelerometers were positioned as described in Figure 5.27, and another accelerometer was positioned on the firewall. The experimental set-up will not be discussed here, since it is very similar to the set-up used in the experiments presented in section 5.2.2, Figure 5.14. Three configurations were investigated. First, control was performed with one actuator and one sensor located on the passenger side of the car. Second, two actuators and two error sensors were positioned as described before (i.e. the two sources are located in the two front doors, and the two error sensors are located at the position of the head of the driver and passenger). Third, an extra error microphone was added in the center of the car.

The response measured with one microphone located at the position of the head of the passenger is shown in Figure 5.31. The microphone signal was band pass filtered between 100 and 450 Hz. The solid blue line shows the sound pressure level before control. It is obviously highly dominated by the harmonics of a low fundamental frequency, 10 Hz, which corresponds to the rotation frequency of the 0.4-meter diameter roller at 53 mph. Figure 5.31 also shows that as the frequency increases, the amplitudes of the harmonics also increase. In fact, the noise inside the cabin due to the roller is very different than the noise measured when the car was driven on a coarse road (section 5.3.1).

Figure 5.31 shows the response at the error sensors located on the side of the driver when two control sources and three error sensors were used. The response after control is shown as a solid red line. It shows that the harmonics are lowered down to the level of the background noise of the roller. A maximum attenuation of 15 dB was achieved at 355 Hz, while the global reduction was 3.5 dB on the entire frequency band of the control. Reductions obtained on the passenger side, as well as in the center of the cabin were 1.5 dB over the 40-450 Hz frequency band. The absolute values of the reduction are not very significant since the characteristics of

the frequency response measured at the error sensors are not really representative of the noise caused by the interaction of the road with the tires. For this reason, no discussion will be provided concerning the effects of the system dimensions on the spatial distribution of the sound pressure level before and after control. When the disturbance is multi harmonic, as is the case for the dynamometer, the acoustic modes being excited are not the same as when the disturbance is broad band, as is the case for the car driven on the road. When the car is driven by the roller, the spatial distribution of the sound pressure inside the cabin is therefore not representative of the sound pressure distribution inside the cabin when the car is driven on the road. However, the path followed by the noise is the same. Therefore, this experiment was useful in determining the positions of the reference sensors required to control road noise.

In conclusion, this test showed that with the set of reference signals used good control was achieved at a sensor located at the head of the passenger, while low reductions were obtained at other error sensors. To some extent, this result agrees with the simulation discussed in section 5.3.1 , since it was shown there that control was achievable when the car was driven on a coarse road. The tests showed that active control of noise due to the contact of the front tires with a smooth surface was possible when an optimized set of four error sensors were used.

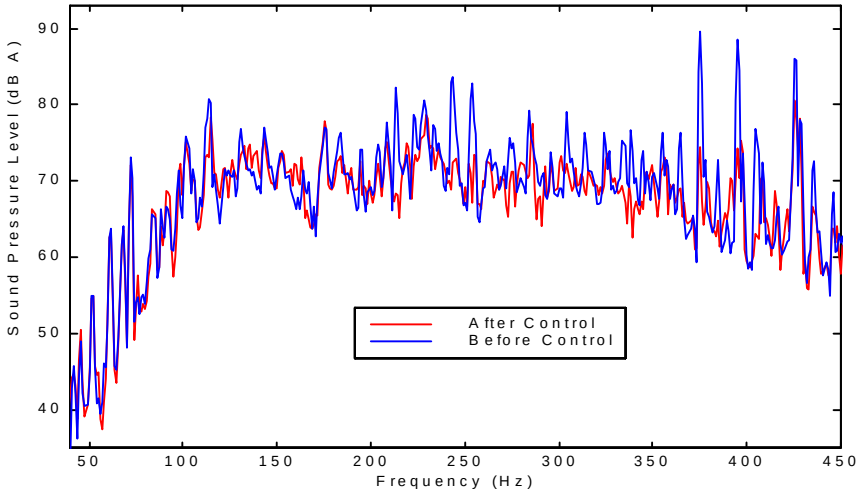

Figure 5.31 SPL at error sensor 1 (head of the passenger)

Figure 5.32 Test rig for the Volvo dynamometer experiment

5.3.3 Simulated road noise

In the previous section, a smooth drum was driving the front wheels of the automobile at a constant speed (53 mph). It was shown that the frequency response measured at a microphone located in the cabin was multi harmonic. The fundamental of the signal occurred at the frequency of rotation of the drum. In this experiment performed at Goodyear in Akron, Ohio, the drum which is driving only the front left wheel is larger (10 feet diameter) and covered with rough aggregate as illustrated in Figure 5.33. The vehicle used to perform the experiments presented in this section is not the VAL vehicle. The VAL equipment was set up on a similar Ford Explorer residing at Goodyear. This is significant since it shows that the system can be readily applied to another vehicle of same type. As a result the sound pressure measured in the cabin is not multi harmonic. In Figure 5.34, the red line shows the response between 40 and 500 Hz measured at one error sensor while the drum is driving one wheel. The figure shows that the signal is broad band. However, most of the energy of the signal is concentrated between 100 and 150 Hz. As discussed in the next section, the response is typical of the response measured in the cabin while the automobile is being driven on a rough road

Figure 5.33 Experimental set-up

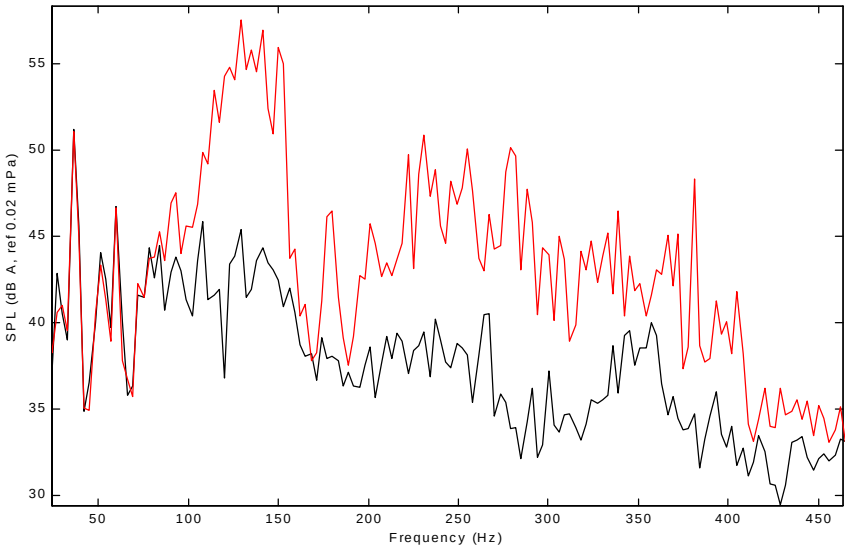

Figure 5.34 Response at error sensor 2

Before discussing active noise control results, the principal component analysis performed while the drum was driving the car will be presented. The experimental set-up is the same as in section 5.3.1 (a). During this test, six accelerometers were fixed to the body of the car. They were equally spaced and located close to the wheel. The response measured at the accelerometers is shown in Figure 5.35. Figure 5.36 shows the singular values between 40 and 1000 Hz. In the entire frequency band, the amplitude of one of the singular value is much larger than the others. It implies that only one independent source of vibration dominates. This is because only one wheel is excited. Therefore, good control of the sound pressure inside the cabin is achievable with a low number of reference sensors. As suggested by Elliott et al [29], two reference sensors (positioned adequately) are required to control the noise due to one source. In section 5.3.1, it was shown that a much larger number of reference sensors were required to obtain reduction of the sound pressure when the car is driven on a coarse road. The main difference with this test comes from the cabin being excited by only one wheel.

The experimental set up used during the active control tests will not be described in detail in this section because it is very similar to the test set up of section 5.3.2. During all the tests, two acoustic sources and two error sensors were used. In a first set of experiments conventional

speakers were used. In a second set of experiments, the piezoelectric speakers were used. In both cases, each error sensor was located at the location of the heads of the driver and passenger.

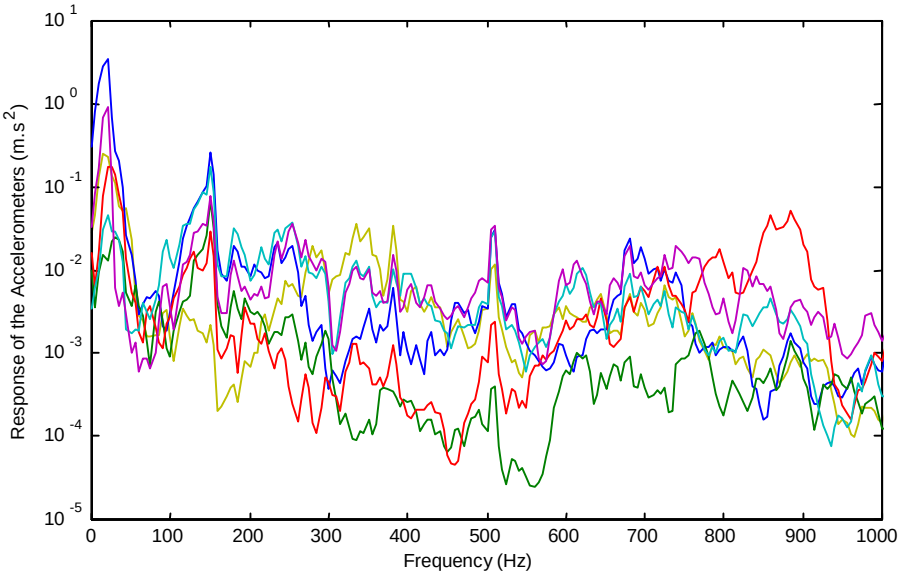

Figure 5.35 Response measured at the accelerometers

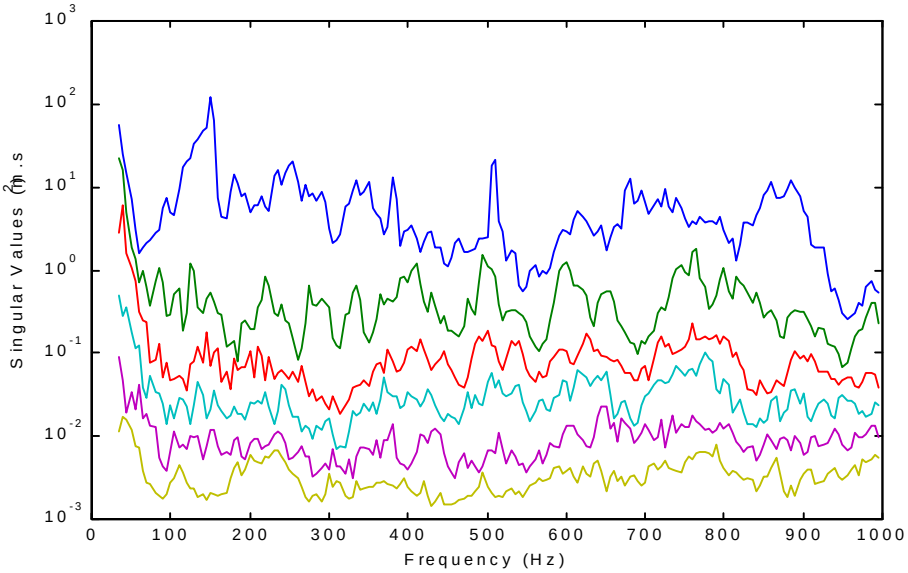

Figure 5.36 Singular values

.

In Figure 5.34, the black line shows the response at error sensor 2 after control. In this configuration, four reference sensors were used. Three were located on the suspension arm in

three perpendicular directions, and one was located on the firewall on the side of the driven wheel. The vibration of the body of the car and particularly the firewall is an important source of noise in the cabin. Due to non linearity that may occur at each connectors that link the wheel to the body of the car, the vibration of the firewall may not be correlated with the vibrations measured close to the wheel. In that case, a reference sensor located on the firewall is necessary to obtain good control. The control sources are the conventional speakers. At error sensor 2, the reduction is over 11 dB in the frequency band of the control (100-500Hz). If the attenuation is computed on a wider frequency band (20-1000 Hz), the reduction is 9 dB. The reduction obtained at error sensor 1 is lower, 9 dB and 6 dB, when computed respectively on the frequency band of control and on the wider band. Note that for frequencies above 1000 Hz, the response is much lower and therefore does not contribute much to the global response.

The case where the control is performed with piezoelectric sources is presented in Figure 5.37. The test set up was kept the same, and only the sources were changed. The reduction obtained in the 100-500 Hz frequency band is low compared to the reduction achieved with conventional speakers. The sound pressure level was decreased by only 2.5 dB in this frequency band. As illustrated in Figure 5.37, no control was achieved below 200 Hz. Poor results at low frequency are due to the dynamics of the source. As discussed in appendix B the output of the source is low at frequencies below 200 Hz. However, control achieved above 200 Hz is very similar to control achieved with conventional speakers. Reduction of 7.2 dB was achieved at error sensor 1 between 200 and 400 Hz.

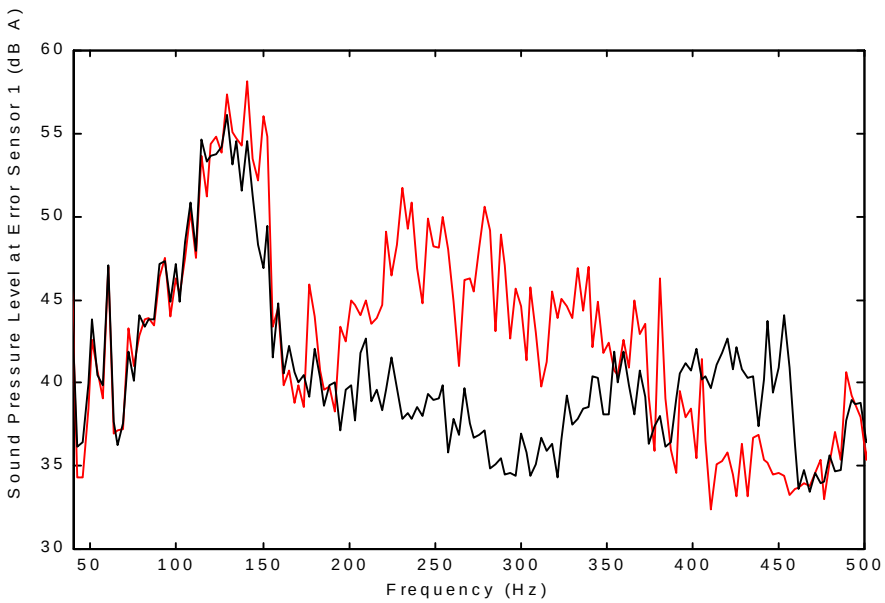

Figure 5.37 Results obtained with the piezoelectric sources

Different combinations and number of reference sensors were investigated. Three accelerometers were positioned in three perpendicular directions on the control arm of the left front wheel as close from the wheel as possible. One accelerometer was located on the firewall on the side of the driver. One microphone was located just behind the turning wheel in order to measure the noise due to the interaction of the road with the tire. The results are presented in Table 5.7 and Figure 5.38. Table 5.7 shows the attenuation of the sound pressure level at the error sensors. The attenuation has been computed for two frequency bands, the control band (100 to 500 Hz) and a larger band (20 to 1000 Hz). The larger band has been chosen because above 1000 Hz the energy associated with the noise due to the contact of the tire with the roller is low compared to the response at frequencies below 1000 Hz. The ear is not sensitive to noise below 20 Hz therefore estimating the attenuation between 20 and 1000 Hz is close to estimating the attenuation in the entire audible frequency range (20 Hz to 20 kHz). Table 5.7 shows that best results are obtained when four reference sensors were used (three accelerometers on the control arm and one on the firewall). In this case the attenuation measured at error sensor 2 is 12.1 dB (9 dB at error sensor 1) in the control band and 9 dB between 20 and 1000 Hz. Figure 5.38 shows that most control is obtained between 100 and 350 Hz. At higher frequency no control was achieved. Table 5.7 shows that very similar attenuation is obtained at error sensors 1 and 2 with three reference sensors. In the configuration presented in the table, three

accelerometers were located in three perpendicular directions on the control arm. As seen in Figure 5.38, the reduction between 260 and 300 Hz is slightly different in the configuration with three reference sensors compared to the configuration involving four reference sensors. At all other frequencies, the response after control is the same in both cases. It means that the non linearity in the path from the wheel to the firewall can be neglected.

Table 5.7 also shows results obtained with four configurations of two reference sensors. The attenuation obtained at the error sensor is different for each configuration. Best results were obtained when the accelerometers were mounted on the control arm in the x direction (transversal motion of the wheel) and z direction (vertical motion of the wheel). In that configuration the attenuation is the same as in the case where three reference sensors were used. It can be seen in Figure 5.38 that the frequency responses after control are very similar too. However, when other combinations of reference sensors were used the attenuation measured at error sensor 2 was lower. For example, when the signal from the microphone and the accelerometers located on the firewall were used (configuration 4) the attenuation measured at error sensor 2 in the frequency band of control was only 5.8 dB. Note from Table 5.7 that when one reference sensor (z-axis on the control arm) was used the reduction measured at error sensor 2 was 6 dB.

Table 5.7 Reduction at the error sensors for various numbers of reference sensors

	Control Band 100 - 500 Hz		20 - 1000 Hz	
	mic 1	mic 2	mic 1	mic 2
4 references	9.0	12.1	6.0	9.0
3 references	9.1	11.7	6.0	9.0
2 references (1)	6.5	8.2	4.9	6.7
2 references (2)	8	11.7	5.9	8.8
2 references (3)	5.3	7.7	4.2	6.1
2 references (4)	4.6	5.8	3.7	5
1 reference	3.7	6.3	3.1	5.4

The experiment presented in this section showed that active control of simulated road noise was possible using two reference sensors carefully positioned, two error sensors and two

control sources. These results agree with those of the principal component analysis, where it was stated that good control was achievable with a number of reference sensors as low as two.

Best results were obtained with conventional speakers. The piezoelectric sources performed well at frequencies above 200 Hz. The reduction obtained with those sources was low compared to the reduction obtained with the conventional speakers, because most of the energy of the signal from the error sensors was between 100 and 150 Hz. When the car is driven on a road, assuming that the disturbances caused by each wheel are not correlated, the controller would require eight reference sensors. However, if it is assumed that the noise measured in front of the car is mainly due to the front wheels, then noise control can be achieved at the position of the driver and front passenger with only four reference sensors.

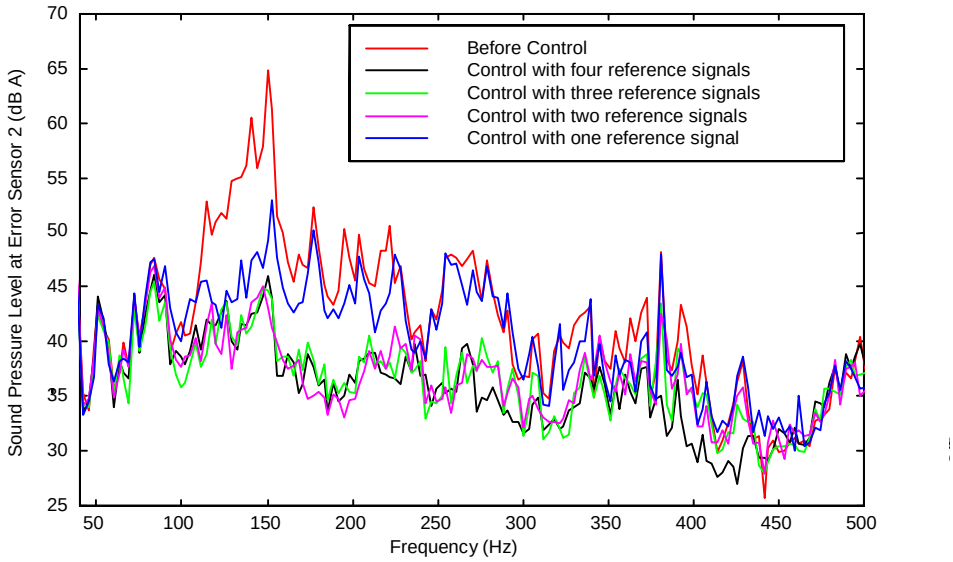

Figure 5.38 Active control in terms of the number of reference sensors

5.3.4 Results obtained on the Road

This section covers the application of active control to real road noise in the Ford Explorer. For this experiment the car was driven on a coarse road at a constant speed of 30 mph. In order to reduce the power train noise inside the automobile cabin, the automobile was driven downhill.

Four reference signals were used. Three reference accelerometers were positioned on the control arm as described in Figure 5.27, and one was located on the firewall on the side of the passenger. One control source and one error sensor were used. As was shown in section 5.3.2, this choice of reference sensor location is better for control of noise on the side of the passenger. Thus, the control source was located in the right front door while the error sensor was placed at the location of the passenger's head.

The control was performed between 100 and 200 Hz. Recall from section 5.3.1 that control in this frequency band was achievable with four reference accelerometers. As was shown in Figure 5.28 (c) the noise level in this frequency band is high. Thus the input and output signals of the controller were band pass filtered between 100 and 200 Hz. In terms of signal processing involved in the controller, the signals were sampled at 1500 Hz, and FIR filters were used to model the path between the actuator and the error sensor as well as the control path. FIR filters were used to ensure the stability of the algorithm. 150 coefficients were used for the system identification, and 220 coefficients were used for the controller. The impulse response between the control source and the error sensor quickly decayed to zero. At a sampling frequency of 1500 Hz, 150 coefficients were sufficient to model the dynamics of the path between the source and the error sensor. Under these conditions, only 220 coefficients can be used for the control path. This limitation is due to the hardware of the present VAL controller. If more coefficients are used, the controller can not handle the signal processing and the update equations in the feedforward algorithm.

Surface roughness is not constant on a typical road. Therefore, the sound pressure level measured inside the cabin varies as the car is driven along the road. In order to overcome this problem the test was performed as follows. The car was driven on the test road with the controller off, and five sets of data were acquired. Each set of data consisted of a ten second time history sampled at 2000 Hz and measured at the error sensor. The frequency response at the error sensor was computed for each set of data with ten averages. In a second step, the car was driven as closely as possible on the same road section with the controller on. Five sets of data were acquired (same sets as when the controller is off). The acquisition was performed such that each set of data, controller on and off corresponds to the same road patch: acquisition of set one with the controller on or off was started as the car was driven along the same path, then

acquisition of set two was started as the car was driven along another path, it being the same with the controller on or off.

In Figure 5.39, the sound pressure level measured at the error sensor is shown before control as a solid blue line and after control as a solid red line. The response shown has been linearly averaged over the five sets of data acquired along the test road. The frequency response is computed over 50 seconds (data sets of 10 seconds each) with 50 samples of 1 second. The data have been averaged in order to reduce the effects of the road surface and car speed variations. The averaging procedure ensures that the attenuation shown in Figure 5.39 is caused by the effects of the controller only.

Most of the control is obtained between 100 and 130 Hz, with a maximum attenuation of 5.4 dB at 105 Hz. The reduction in the frequency band is 2.3 dB, while it is 3 dB between 100 and 130 Hz.

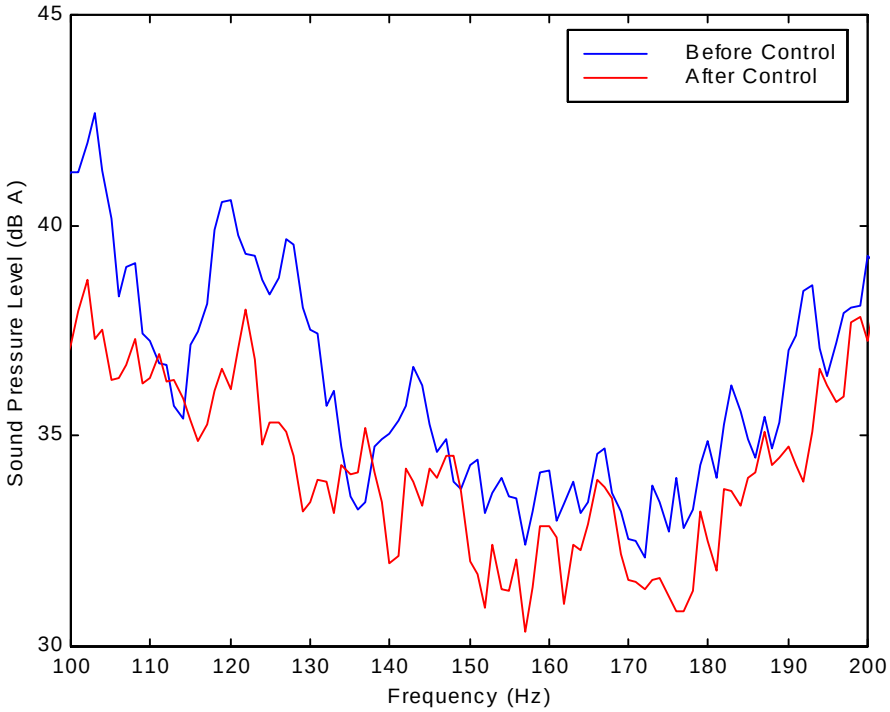

Figure 5.39 Averaged sound pressure level (dB A) at error sensor

In Figure 5.40, the response is shown before and after control over the first part of the road, which corresponds to data set 1. In this case, the maximum attenuation was 8 dB, obtained

at 105 Hz. Attenuation close to 5dB was obtained between 100 and 130 Hz. In the entire frequency band a total reduction of 4 dB was obtained.

The conclusions are not straightforward. It was shown that a reduction of 2 dB in cabin noise is possible when the car was driven on a coarse road. It is difficult to provide any significant conclusions concerning the maximum reduction measured on the road. Two parameters, which influence the sound pressure level in the cabin, were not fully controlled in the experiment. First, the speed of the vehicle might have varied by as much as a couple of miles per hour between any two sets of data. Second, it was not guaranteed that the automobile was driven on the same exact road patch. Clearly, the path of the automobile may have shifted right or left during the numerous passages of the car over the same portion of the road. It see, reasonably to conclude that the car was not driven on a road patch with the same roughness at each passage. This change in surface roughness modifies the sound pressure measured in the cabin.

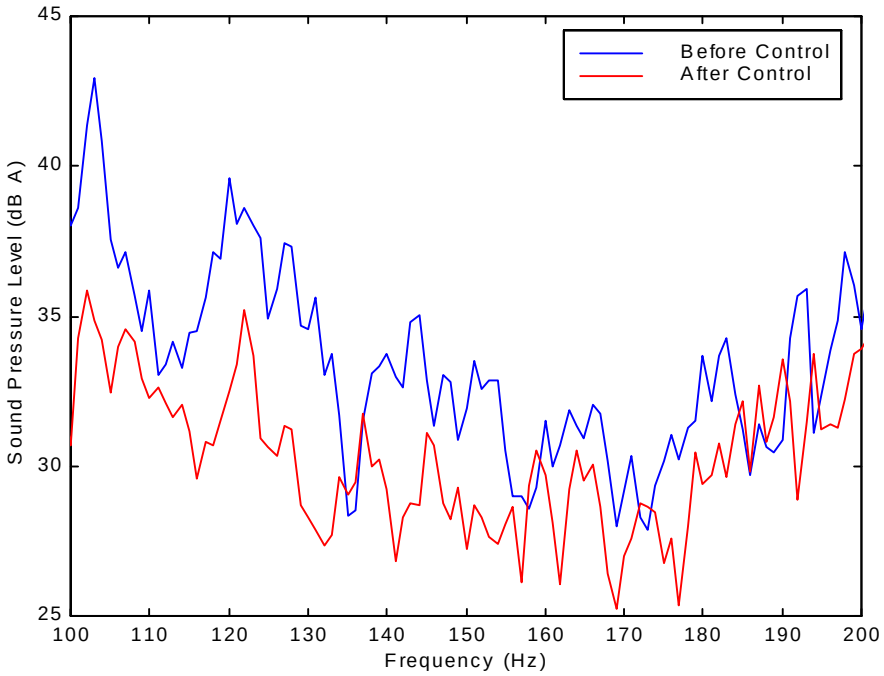

Figure 5.40 Sound pressure level (dB A) at error sensor. Set 1

5.3.5 Conclusions

In this section, it was shown that active control of road noise is feasible when the automobile is driven on a coarse road. Investigation of the choice of reference signals showed that very good control should be achievable using eight reference signals in a larger band, from 40 to 500 Hz. Because of hardware limitations the system presented in this section used only four reference sensors. After optimization of the four reference sensor locations, it was shown that the achievable noise reduction was only two decibel lower than the noise reduction achievable with six reference sensors located in three perpendicular directions on the front right wheels.

Results obtained on a dynamometer with the optimized configuration of four references showed that the reduction was higher on the side of the passenger than on the side of the driver or in the center of the cabin.

Noise attenuation of two to four decibel was obtained at the error sensor, in the 100-200 Hz frequency band. These results were obtained with a system composed of four reference sensors, one secondary source and one error sensor located on the side of the passenger.